

AD-A049 573

ROYAL AIRCRAFT ESTABLISHMENT FARNBOROUGH (ENGLAND)  
METHODS FOR PREDICTING SATELLITE ORBITAL LIFETIMES. (U)  
JUL 77 D G KING-HELE

F/G 22/3

UNCLASSIFIED

| DF |  
AD  
A049573  
REF

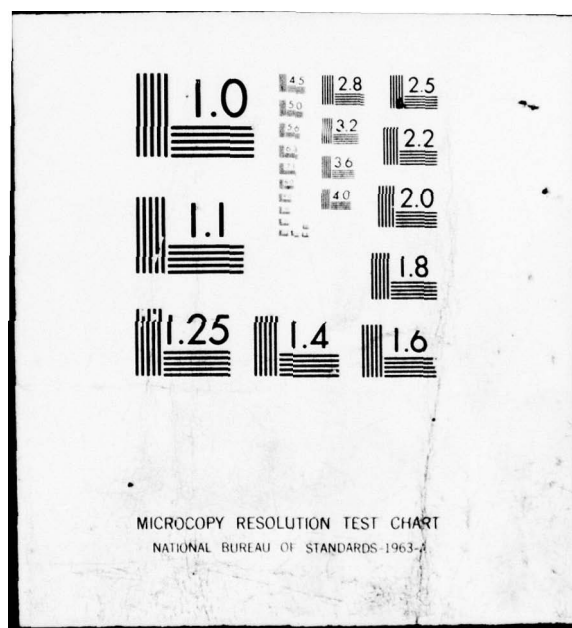
RAF-TR-77111

DRIC-RR-59173

NL



END  
DATE  
FILED  
3 - 78  
DDC



AD A 049573 TR 77111

TR 77111

UNLIMITED

BR59173



ROYAL AIRCRAFT ESTABLISHMENT

\*

Technical Report 77111

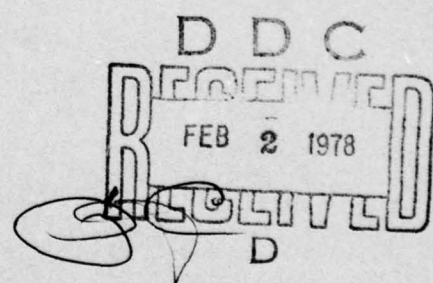
July 1977

METHODS FOR PREDICTING  
SATELLITE ORBITAL LIFETIMES

by

D.G. King-Hele

\*



Procurement Executive, Ministry of Defence  
Farnborough, Hants

UNLIMITED

ACCESSION NO.	
WHITE SECTION	WHITE SECTION <input checked="" type="checkbox"/>
BLACK SECTION	BLACK SECTION <input type="checkbox"/>
REFINISHED	
JUSTIFICATION	
BY	
DISTRIBUTION/AVAILABILITY CODES	
DISL	AVAIL. AND/or SPECIAL
A	

(18) DRIIC

(19) BR-59173

UDC 521.6 : 521.4 : 629.19.077.3

(14) RAE-TR-77111

ROYAL AIRCRAFT ESTABLISHMENT

(9) Technical Report 77111

Received for printing 28 July 1977

(11) Jul 77

(12) 56p

(6) METHODS FOR PREDICTING SATELLITE ORBITAL LIFETIMES,

by

(10) D. G. King-Hele

#### SUMMARY

The accurate prediction of satellite decay dates some months or years ahead remains one of the most difficult and intractable problems of orbital mechanics, chiefly because the lifetime depends strongly on the future variations in air density, which are at present not accurately predictable.

In this paper simple graphical methods are presented for estimating the future lifetime of an Earth satellite from its current rate of decay, using theory adapted to an atmosphere with a realistic variation of density with height. The effects of the departure of the Earth and atmosphere from spherical symmetry, and the variations of density with time, are approximated by specifying correction factors. Orbits which experience serious lunisolar perturbations call for numerical-integration methods, and the uses of the computer programs PROD and PTDEC are described.

Despite the many uncertainties, the remaining lifetimes of most satellites should be predictable with an accuracy of  $\pm 10\%$  by these methods, which are based on many years' experience in making the monthly decay predictions for the RAE Table of satellites.

Departmental Reference: Space 532

Copyright

©

Controller HMSO London  
1977

D D C  
REF ID: FEB 2 1978  
R  
REGULATED  
D

310450

Done

LIST OF CONTENTS

	<u>Page</u>
1 INTRODUCTION	3
2 DEVELOPMENT OF APPROXIMATE THEORY	5
2.1 Assumptions	5
2.2 Variation of $H$ with height	6
2.3 Formulae for lifetime	6
3 RESULTS	7
3.1 Over the full range of $e$	7
3.2 For $0 < e < 0.03$	8
3.3 For $0.03 < e < 0.2$	9
3.4 For $0.2 < e < 0.8$	10
4 CORRECTIONS TO THE RESULTS	10
4.1 Introduction	10
4.2 Variation of perigee height	10
4.3 Atmospheric oblateness	12
4.4 The future variations of air density	12
4.4.1 Variations over the 11-year solar cycle	13
4.4.2 Satellites with lifetimes of several solar cycles	13
4.4.3 The day-to-night variation	16
4.4.4 The semi-annual variation	17
4.4.5 Irregular day-to-day variations	18
4.5 Envoi	18
5 PROCEDURES WHEN LUNISOLAR PERTURBATIONS ARE LARGE	18
5.1 The PROD program	18
5.2 Calculation of perigee height from decay rate	20
5.3 The PTDEC program	21
5.4 Decrease in drag coefficient at low altitudes	23
6 CONCLUDING REMARKS	24
References	25
Illustrations	Figures 1-26
Report documentation page	inside back cover

1 INTRODUCTION

Most satellites decay because of the unceasing attrition of their orbits by air drag, and their remaining lifetimes depend on the future variations in air density, which cannot yet be predicted accurately. So lifetime prediction is inevitably an inexact art: the accuracy is rarely better than  $\pm 10\%$ , and sometimes considerably worse. Although lifetime prediction may seem to be a losing battle, this is no excuse either for an ignominious retreat or for the use of inaccurate theory, which would add significant bias errors to the inevitable random errors. The present Report describes the simple graphical methods developed at RAE, based on theory accurate to about 2%, and the numerical-integration methods used when lunisolar perturbations are large enough to invalidate the simple techniques.

"Why make lifetime estimates?", you may ask. The answers are various. For scientific satellites the scheduling of experiments may need to be changed if, for example, the orbital lifetime proves to be six months instead of the twelve months planned; or the experimenters may have to estimate the latest possible date for firing an on-board rocket to avoid premature decay, or decide whether a satellite will still be in orbit at the time of some intensive observation campaign, such as the International Magnetospheric Study of 1978 - if not, a replacement satellite might have to be launched. The predicted lifetime also strongly influences the choice of satellites for observation and orbital analysis over their complete life: the amount of analysis and observing required is very different if the lifetime is five years rather than two years. When a satellite is approaching decay, the date of decay needs to be known in advance if plans are to be made for intensive observation during the last few weeks of the life, for either scientific or military motives. The need for accurate decay predictions is particularly acute for optical observations, because the periods of visibility for optical observation may last for as little as a week, and a decay prediction accurate to a few days is needed to decide whether the satellite will be visible or unobservable on the day of decay.

Satellites which execute orbital manoeuvres on command are of course outside the scope of this paper.

Lifetime prediction is a thankless task: if your prediction is right, others wrongly think it is easy; and if you are wrong, you earn even less credit. Our commitment to the subject began in 1958 with the compilation of the first RAE Table of satellites recording details of each successful new launch, including estimates of orbital lifetimes. By 1961 the Table had grown

into a ten-page RAE Technical Memorandum<sup>1</sup>, and from then onwards it was issued more frequently: there have been monthly issues for the past twelve years. By the end of 1976 there were three volumes totalling more than 500 pages, covering about 3000 satellites and rockets in detail<sup>2,3</sup>. The lifetime estimates for these satellites and rockets as they near decay have been updated at monthly intervals by Doreen Walker and the author, using methods which have to be very simple, because a great many estimates must be made quickly each month. In developing methods for decay prediction, the main interest is in lifetimes of a few months or a few years: lifetime estimates of more than twenty years are critically dependent on future solar activity, which is at present unpredictable.

In an atmosphere which does not vary with time, the remaining lifetime  $L$  of a satellite in an orbit of eccentricity  $e$  may be expressed in terms of the mean motion  $n$  and its rate of change  $\dot{n}$ . The simplest theory gives

$$L = \frac{3en}{4\dot{n}} , \quad (1)$$

for eccentricities between 0.03 and 0.2. This was the equation first used in 1957, but improved versions were soon derived<sup>4</sup>, and also equations applicable for lower and higher eccentricities, and for an oblate atmosphere<sup>5-7</sup>.

Strangely enough, despite the huge advances in space science and technology in the past twenty years, it is still best to use an equation of this type, with an observational value of  $\dot{n}$ , because the masses and sizes of about 90% of newly-launched objects are not revealed by the launching authorities. In 1976 this information was not available on the 99 Russian launches and the 12 US military launches; most of the remaining 17 launches were of satellites which entered high orbits, and lifetime estimates were not of much interest.

Although most satellites decay because their total energy is whittled away by air drag over months or years, there is an important class of orbits - those with eccentricities between 0.7 and 0.8 - for which the lifetime is controlled by the perturbations in the perigee height due to lunisolar gravitational attraction. These perturbations can alter the perigee height by more than 1000 km in a few years, and can bring the perigee down to heights near 100 km, where rapid or catastrophic decay occurs. The most important satellites in this class are the Russian Molniyas and their rockets, of which more than 100 have been launched. For these satellites we rely upon numerical integration of the lunisolar perturbations, backed up by approximate theoretical methods. The

numerical-integration methods could of course be used for all satellites, but the computer time required would be prohibitive.

Sections 2 to 4 of this Report deal with the estimation of lifetime by quick and simple graphical methods, for 'normal' decay under air drag. Section 5 deals with high-eccentricity orbits subject to strong lunisolar perturbations, and describes the use of the computer programs PROD (drag-free) and PTDEC (with drag included).

## 2 DEVELOPMENT OF APPROXIMATE THEORY

### 2.1 Assumptions

In developing theory for the effect of air drag on satellite orbits, it is simplest to assume a spherical Earth with a spherically symmetrical atmosphere which does not vary with time, and has a density  $\rho$  varying exponentially with height  $y$ , so that

$$\rho = \rho_0 \exp\{-(y - y_0)/H\} \quad , \quad (2)$$

where suffix 0 denotes a convenient reference height (usually taken as perigee height) and  $H$ , the 'density scale height', is taken as constant. If we write  $z = ae/H$ , where  $a$  is the semi major axis of the orbit, the remaining lifetime of the satellite can, under these simple assumptions, be expressed in terms of  $n$  as<sup>6</sup>

$$L = \frac{3en}{4n} \left\{ 1 + \frac{7e}{6} + \frac{5e^2}{16} + \frac{1}{2z} \left( 1 + \frac{11e}{12} + \frac{3}{4z} + \frac{3}{4z^2} \right) + O\left(e^3, \frac{1}{2z^4}\right) \right\} \quad , \quad (3)$$

for  $0.03 < e < 0.2$ . Within these limits for  $e$ , the value of  $z$  is usually between 3 and 40, so that the neglected terms in (3) never exceed 1%. Similar formulae can be derived<sup>5,7</sup> for  $e < 0.03$  and  $> 0.2$ .

In practice, equation (3) needs correction because (a) the density does not vary exponentially with height; (b) the upper atmosphere and the Earth are appreciably oblate; (c) the perigee height varies as a result of perturbations from odd zonal harmonics in the geopotential; and (d) the density does not remain constant but varies on daily, monthly, semi-annual and 10 yearly time-scales, due to solar activity and other effects (for a review, see Ref 8). These variations in density, often by a factor of 2 and sometimes by a factor of up to 10, make accurate estimates of lifetimes impossible. Nevertheless it is reasonable to aim for an accuracy of about 10% for lifetimes of less than one year.

The methods of lifetime estimation presented here make full allowance for correction (a), while separate correction factors are specified in section 4 for corrections (b), (c) and (d).

## 2.2 Variation of H with height

If we define the scale height  $H$  as  $\left(-\frac{1}{\rho} \frac{dp}{dy}\right)$  and assume that  $H$  varies linearly with height, having a gradient  $dH/dy = \mu$ , it is found from a recent revision of Ref 9 that the extra terms to be added inside the curly brackets in equation (3) are

$$- \mu \left( \frac{1}{4} - \frac{1}{2z} \right) + O(\mu^2) . \quad (4)$$

In the real atmosphere  $\mu$  is not constant, but a constant value appropriate to the initial perigee height will serve, because the perigee height decreases by only about  $\frac{1}{2}H$  during the first 90% of the life<sup>5</sup>.

Fig 1 shows the variation of  $H$  and  $dH/dy$  as given<sup>10</sup> by the COSPAR International Reference Atmosphere 1972 for high and low levels of solar activity: the curves are for exospheric temperatures of 1100 K and 800 K respectively, corresponding to solar 10.7 cm radiation energy  $F_{10.7}$  of about 150 and  $80 \times 10^{-22} \text{ W m}^{-2} \text{ Hz}^{-1}$  respectively, at the mean of the day-to-night and semi-annual variations. The 'high solar activity' is approximately the level during the solar maximum of 1968-70, and the 'low' is near the level during the prolonged solar minimum of 1974-76. Although Fig 1 runs from 100 km up to 600 km height, the satellites for which lifetime estimates are required usually have perigee heights between 200 and 400 km: so, if a standard value of  $\mu$  is needed,  $\mu = 0.1$  is a suitable choice.

## 2.3 Formulae for lifetime

On adding the terms (4), we may rewrite equation (3) as

$$L = \frac{3en}{4n} \left\{ 1 + \frac{7e}{6} + \frac{1}{2z} + \frac{3}{8z^2} - \mu \left( \frac{1}{4} - \frac{1}{2z} \right) + O\left(\frac{5e^2}{16}, \frac{3}{8z^3}, \frac{11H}{24a}, \mu^2\right) \right\} \quad (5)$$

for  $e < 0.2$  and  $z > 3$  ( $e$  greater than about 0.03). The maximum values of the 0 terms in (5) are 0.012 (when  $e = 0.2$ ), 0.014 (when  $z = 3$ ), 0.005 (if  $H = 70$  km), and 0.01 (if  $\mu = 0.1$ ): these maximum errors do not occur simultaneously, and the total error due to approximations in the theory may be assessed as 2%. 111

For  $z < 3$ , the appropriate formula for lifetime is<sup>9</sup>

$$L = \frac{3enI_0(z)}{4\dot{n}I_1(z)} \{1 - \mu J + O(e^2, \mu)\} \quad (6)$$

where  $J$ , given in Fig 14 of Ref 9, decreases almost linearly from 1.0 at  $z = 0$  to 0.2 at  $z = 1.2$  and is of order 0.1 for  $1.5 < z < 3$ . The functions  $I_0$  and  $I_1$  in (6) are Bessel functions of the first kind and imaginary argument, of degree 0 and 1, and argument  $z$ . For circular orbits ( $z \rightarrow 0$ ), equation (6) reduces to

$$L = \frac{3Hn}{2a\dot{n}} (1 - \mu) \quad . \quad (7)$$

For  $e > 0.2$ , the lifetime may be taken as

$$L = \frac{en}{\dot{n}} F(e) (1 - \frac{1}{4}\mu) \quad , \quad (8)$$

where  $F(e)$  is plotted in Fig 4.10 of Ref 11, and the  $\mu$  term is carried over from equation (5), the  $\mu/2z$  term being negligible for  $e > 0.2$  ( $z > 40$ ). The theory for  $e > 0.2$  in an atmosphere in which  $H$  varies with height has not yet been fully developed, but the assumption that the correction factor is  $(1 - \frac{1}{4}\mu)$  is unlikely to cause significant errors.

### 3 RESULTS

#### 3.1 Over the full range of $e$

In presenting the results it is convenient to write

$$L = Q/\dot{n} \quad (9)$$

and to give values of  $Q$ . Fig 2 shows how  $Q$  varies with  $e$  for perigee heights of 200 km (full lines) and 300 km (broken line) for high and low solar activity over the whole range of  $e$  from 0 to 0.8. Over most of this range the curves for perigee heights of 200 and 300 km very nearly coincide, and the curves may be taken as applying over the range 200-300 km. In preparing Fig 2, the values of  $Q$  are obtained from equations (5), (6) and (8), using values of  $H$  and  $\mu$  from Fig 1.

The lifetime of any satellite perturbed primarily by air drag may be estimated approximately by reading off  $Q$  from Fig 2 and dividing by the observational value of  $\dot{n}$  (rev/day<sup>2</sup>). It should be remembered, however, that if  $e > 0.4$ , the orbit may be strongly perturbed by lunisolar gravitational attraction: there is no easy way of guessing the magnitude of the lunisolar

perturbations, but it is found in practice that Fig 2 may be useful up to  $e = 0.8$  for low-inclination orbits, while for many high-inclination orbits the graph loses its accuracy for  $e > 0.6$ . In Fig 2 the scale is terminated at  $e = 0.8$ , because lunisolar perturbations seriously affect nearly all orbits with eccentricities greater than 0.8.

The lower end of Fig 2 cannot be read accurately enough for practical use, and sections 3.2 to 3.4 describe more accurate and more detailed graphs (Figs 3 to 10) for the two levels of solar activity and perigee heights between 150 and 600 km.

### 3.2 For $0 \leq e \leq 0.03$

Fig 3 shows the values of  $Q$  for  $e < 0.03$  and a range of values of  $n$ , when  $\mu = 0.1$  and  $H$  has the value given in Fig 1. When  $e < 0.01$ , the value of  $Q$  is more sensitive to perigee height (or  $n$ ) than to  $e$ , and  $Q$  is plotted against  $n$  in Fig 4 for fixed values of  $e$  between 0 and 0.01, again for  $\mu = 0.1$ . (It is more useful to plot  $Q$  against  $n$  rather than against perigee height, because the value of  $n$  is always accurately known, whereas the perigee height is often not available - it is not given explicitly in the USAF 2-line elements, which are widely used in calculating lifetimes.) In Figs 3 and 4, where  $\mu$  has its standard value of 0.1,  $Q$  is given by

$$Q = \frac{3\pi n I_0(z)}{4I_1(z)} \{1 - 0.1J\} \quad (10)$$

from equation (6):  $z = ae/H$  is calculated using values of  $H$  from *CIRA 1972* as given in Fig 1, and the difference between the curves for high and low solar activity is caused by the differences in the values of  $H$ . Values of  $J$  are read from Fig 14 of Ref 9.

The standard value of 0.1 for  $\mu$  in Figs 3 and 4, although convenient when applying further theoretical adjustments, is rather illogical, because the values of  $H$  used are realistic, and vary with height and solar activity. Figs 3 and 4 have therefore been re-calculated and re-drawn using the values of both  $H$  and  $\mu$  given in Fig 1. The results are shown in Figs 5 and 6, which may be regarded as giving values of  $Q$  based on realistic values of both  $H$  and  $\mu$  in the best existing reference atmosphere.

Figs 5 and 6 therefore provide the best set of values for  $Q$  for use in practical estimation of lifetime, though still subject to the errors to be discussed in section 4. The values of  $Q$  are given in rev/day on the assumption

that  $\dot{n}$  is calculated by differencing two values of  $n$  (rev/day) at least a day apart, and dividing by the time interval, to give  $\dot{n}$  in rev/day<sup>2</sup>. The lifetime  $Q/\dot{n}$  is then in days. It is intended that Fig 5 should be used if  $0.01 < e < 0.03$ , and Fig 6 if  $0 < e < 0.01$ .

Fig 5 shows that the influence of solar activity on  $Q$  is greatest when  $e$  is small:  $Q$  is about 25% greater for high solar activity, for  $n < 16$ . This merely reflects the fact that  $H$  is about 25% greater when solar activity is high, for  $y_p > 250$  km (see Fig 1), since  $Q$  is proportional to  $H$  for  $e = 0$  and  $\mu$  is small for  $y_p > 250$  km. Although  $Q$  is greater when solar activity is high, the density is *much* greater, and so therefore is  $\dot{n}$ . Thus the lifetime  $Q/\dot{n}$  is always shorter when solar activity is high.

The differences and peculiarities in the shapes of the curves in Figs 3 to 6 stem from the fact that they embody the variations of  $H$  in Fig 1, while Figs 5 and 6 are also affected by the variations of  $\mu$  in Fig 1. For example, the strong decrease of  $Q$  in Fig 4 as perigee height drops from 300 km to 150 km is a direct result of the strong decrease in  $H$ , from 52 km at 300 km height to 18 km at 150 km height (for high solar activity). This effect is even greater in Fig 6, because of the increase in  $\mu$  as perigee height drops from 300 to 150 km.

### 3.3 For $0.03 < e \leq 0.2$

When  $e$  is within this range of values,  $Q$  increases almost linearly with  $e$  and the most accurate graphical presentation is achieved by writing

$$L = \left( \frac{Q}{e} \right) \dot{n} \quad (11)$$

and plotting  $Q/e$  against  $e$ . The values of  $Q/e$  are given by the right-hand side of equation (5), with a factor  $3n/4$  outside the curly brackets, rather than  $3en/(4\dot{n})$ .

Figs 7 and 8 give the values of  $Q/e$  for perigee heights between 150 and 600 km, for high and low solar activity, with values of  $H$  from Fig 1. In Fig 7 the value of  $\mu$  is taken constant at 0.1, while in Fig 8 realistic values of  $\mu$  are used, taken from Fig 1. Because of the wide scale, accurate values of  $Q/e$  can easily be read from Figs 7 and 8. Since the range of variation of  $Q/e$  is so small, the variations in  $\mu$  (which has a minimum near 400 km) are enough to convert the curves of Fig 7 to an arched form (usually with maxima between 300 and 400 km) in Fig 8. In practice, satellites with lifetimes of a few weeks or months usually have perigee heights between 150 and 300 km, and

Fig 8 shows that the values of  $Q$  are then confined to a very narrow band: at  $e = 0.1$ , for example,  $1.10 < Q < 1.15$  for high solar activity, and  $1.11 < Q < 1.15$  for low solar activity.

### 3.4 For $0.2 \leq e \leq 0.8$

The value of  $Q$ , now given by equation (8), is plotted against  $e$  for  $\mu = 0.1$  in Fig 9, for perigee heights of 200, 400 and 600 km: the variation with perigee height is linear. Fig 10 shows the values of  $Q$  when  $\mu$  has the *CIRA* values of Fig 1, for perigee heights between 150 and 600 km. With these realistic values of  $\mu$ , there is little variation of  $Q$  with perigee height for perigee heights between 150 and 500 km. When  $e > 0.4$ , Fig 10 should be used with caution, because the orbit may suffer significant perturbations in perigee height due to lunisolar gravitational effects. If these perturbations are less than about 50 km, it may still be possible to use Fig 10, if the value of  $\dot{n}$  can be averaged over a cycle of the lunisolar perturbation; but if the perturbations are larger than 100 km, numerical-integration methods are needed (see section 5).

## 4 CORRECTIONS TO THE RESULTS

### 4.1 Introduction

Figs 5, 6, 8 and 10 provide values of  $Q$  in an atmosphere with realistic values of  $H$  and  $\mu$ , for all values of  $e$  and perigee heights between 150 and 600 km. These graphs would give accurate lifetimes if the Earth and atmosphere were spherical and the density did not vary with time. These ideal conditions do not apply in practice, and several corrections are necessary, which will now be described, although they are not easily presented in graphical form.

### 4.2 Variation of perigee height

One important correction arises because in practice the perigee height  $y_p$  varies with the argument of perigee  $\omega$ . If we write

$$y_p = r_p - R_p \quad , \quad (12)$$

where  $r_p$  is the perigee distance from the Earth's centre and  $R_p$  the local Earth radius, the variation in  $y_p$  arises from (a) the variation of  $r_p$ , due mainly to the effects of odd zonal harmonics in the geopotential, and (b) the variation of  $R_p$  with latitude. In terms of the argument of perigee  $\omega$ , the variation in  $r_p$  is of the form

$$r_p - r_{p0} = -a\beta \sin \omega + (\Delta r_p)_2 + (\Delta r_p)_{LS} \quad , \quad (13)$$

where  $a\beta$  is the amplitude of the oscillation due to odd zonal harmonics, given in Fig 11 of Ref 12, and of order 10 km for most inclinations; and suffix 0 denotes a reference value, chosen to be where  $\omega = 0$ . The quantity  $(\Delta r_p)_2$  is the amount<sup>13</sup> by which  $r_p$  differs from  $a(1 - e)$ ; it is usually of order 1 km and will be ignored here.  $(\Delta r_p)_{LS}$  is the lunisolar perturbation<sup>14</sup>, which is usually less than 1 km for orbits with  $e < 0.4$  and will also be ignored: if  $(\Delta r_p)_{LS}$  is large, numerical-integration procedures have to be used (see section 5). The decrease in  $r_p$  due to air drag is allowed for in the lifetime formulae and need not be considered. The local Earth radius at perigee,  $R_p$ , may be expressed as

$$R_p = 6378.1 - 21.4 \sin^2 i \sin^2 \omega \quad \text{km} \quad . \quad (14)$$

Hence, if  $y_{p0}$  is the value of  $y_p$  when  $\omega = 0$ , equations (12) to (14) give

$$y_p - y_{p0} = 21.4 \sin^2 i \sin^2 \omega - a\beta \sin \omega \quad \text{km} \quad . \quad (15)$$

The variation of  $y_p$  with  $\omega$  for a variety of inclinations  $i$  is shown in Fig 11. (The values of  $a\beta$  used in Fig 11 are from Ref 15: more recent values<sup>12</sup> are within 1 km except near  $i = 10^\circ$ .)

The best method of allowing for the variation of  $y_p$  with  $\omega$  is to modify the current value of  $\dot{n}$  so that it becomes the value,  $\dot{\bar{n}}$ , say, that  $\dot{n}$  would have if the current value of  $y_p$  were equal to its mean value  $\bar{y}_p$  during the subsequent lifetime (again excluding the decrease due to air drag). Since  $\dot{n}$  is proportional to  $r_p$ , equation (2) gives

$$\dot{\bar{n}} = \dot{n} \exp \{ (y_p - \bar{y}_p) / H \} \quad , \quad (16)$$

where  $H$  is given in Fig 1.

If the argument of perigee is expected to move through several revolutions before decay, equation (15), averaged over a cycle of  $\omega$ , gives

$$\bar{y}_p = y_{p0} + 10.7 \sin^2 i \quad \text{km} \quad , \quad (17)$$

so that, from (16),

$$\dot{\bar{n}} = \dot{n} \exp \{ (y_p - y_{p0} - 10.7 \sin^2 i) / H \} \quad . \quad (18)$$

So the best plan is to read off  $(y_p - y_{p0})$  from Fig 11 and  $H$  from Fig 1, and take the lifetime as  $Q/\dot{\bar{n}}$ , where  $\dot{\bar{n}}$  is given by (18). Alternatively, to avoid this correction,  $\dot{n}$  may be evaluated when  $(y_p - y_{p0})$  is within 1 km of its mean

value  $10.7 \sin^2 i$  (indicated on the right of Fig 11). For  $i = 90^\circ$ , for example, this would mean that  $\dot{n}$  should be evaluated when  $\omega$  is within the ranges:  $68-82^\circ$ ,  $98-112^\circ$ ,  $208-214^\circ$  or  $326-332^\circ$ . Fig 12 shows how these 'safe' values of  $\omega$ , where no perigee height correction is needed, vary with  $i$ : the 'safe areas' are stippled. The safest values of  $\omega$  are in the northern hemisphere and generally not far from  $90^\circ$ . For  $20^\circ < i < 55^\circ$ , the best value of  $\omega$  is  $90^\circ$ ; for  $68^\circ < i < 90^\circ$ , a good simple rule is to take  $\omega = i - 10^\circ$  (or  $190^\circ - i$ ); for  $55^\circ < i < 68^\circ$ , the only safe values of  $\omega$  are two narrow bands, in the southern hemisphere near  $205^\circ$  and  $335^\circ$  for  $55^\circ < i < 62^\circ$ .

If the argument of perigee is expected to travel through less than about  $1\frac{1}{2}$  revolutions before decay, *i.e.* if  $L\dot{\omega}$  is less than about  $540^\circ$ , the mean value of  $(y_p - y_{p0})$  in the remaining life may be estimated graphically from Fig 11. The difference between the current value of  $(y_p - y_{p0})$  and this mean value  $(\bar{y}_p - y_{p0})$  is substituted into (16) to give  $\dot{n}$  and hence  $L = Q/\dot{n}$ . It is not always easy to estimate the mean value of  $(y_p - y_{p0})$  from Fig 11, and it is useful to note that  $10.7 \sin^2 i$  is the mean value between  $\omega = 90^\circ$  and  $\omega = 270^\circ$ , as well as over a whole cycle. In practice an iterative procedure may be needed:  $L$  is first calculated using (18); but if it then turns out that  $L\dot{\omega} < 540^\circ$ , a recalculation of  $\bar{y}_p$  is necessary, leading to a revised value of  $L$  from (16).

#### 4.3 Atmospheric oblateness

The correction specified in section 4.2 tacitly takes account of the main effects of atmospheric oblateness, because of the underlying assumption that the density depends on the height  $y_p$  above an oblate Earth. This is equivalent to assuming that the constant-density surfaces are oblate, and of ellipticity  $\epsilon \approx 0.0033$ . However, the theory<sup>6</sup> indicates a further small change in the lifetime formula, by a factor  $\left\{1 + \frac{\epsilon r_p I_2(z)}{2H\dot{\omega}_0(z)} \sin^2 i \cos 2\bar{\omega}\right\}$  for  $z < 5$ , and  $\left\{1 + \frac{2\epsilon}{e} \sin^2 i \cos 2\bar{\omega}\right\}$  for  $z > 5$ . Here  $\cos 2\bar{\omega}$  is the mean value of  $\cos 2\omega$  in the remaining lifetime. The changes due to this factor can be as much as 10% for polar orbits with  $\cos 2\bar{\omega} \approx 1$  and  $z \approx 5$ ; but these conditions are most unlikely to occur simultaneously and for an 'average' orbit, with  $i \approx 45^\circ$ ,  $\cos 2\bar{\omega} \approx \frac{1}{2}$  and  $z \approx 10$  (or 1), the change is 2%. In view of the much larger possible errors due to variations in air density, this correction is rarely worth making.

#### 4.4 The future variations of air density

This is by far the largest source of error, and a very intractable one. The variations are considered here under four headings: solar-cycle, day-to-night; semi-annual; and irregular day-to-day.

#### 4.4.1 Variations over the 11-year solar cycle

Fig 13 shows the variation of density with height by day and by night at a typical sunspot maximum and minimum<sup>8</sup>. At heights near 600 km the density varies by a factor of 20 during the sunspot cycle, with corresponding changes in satellite decay rates. At present neither the intensity nor the date of a sunspot maximum can be predicted accurately, so lifetime estimates can only take account of solar-cycle variations in a very approximate way. Lifetime estimates are most often made for satellites with perigee heights between 200 and 300 km, and for these satellites the variation in density during a solar cycle is less, the ratio of maximum/minimum density being between 2 and 5.

If the satellite is expected to remain in orbit for several solar cycles, and a fairly accurate value of  $\dot{n}$  is available, the lifetime  $L$  may be taken as

$$L = \frac{9}{\dot{n}} \left( \frac{\rho_p}{\bar{\rho}_p} \right) , \quad (19)$$

where  $\rho_p$  is the current density at perigee height, and  $\bar{\rho}_p$  is its mean value over a solar cycle. If the variation of solar activity with time during a solar cycle has a sinusoidal form - admittedly not always a good approximation - we may take  $\bar{\rho}_p = \frac{1}{2}(\rho_{p\min} + \rho_{p\max})$ , where 'min' and 'max' denote values averaged over day and night at the minimum and maximum of the cycle. Values of  $\bar{\rho}_p$ , taken as the arithmetic mean of the CIRA values for exospheric temperatures of 800 and 1100 K, are plotted as a broken line in Fig 13: it nearly coincides with the night-time solar maximum curve. For a perigee height of 300 km, the correction factor  $\rho_p/\bar{\rho}_p$  is between 0.2 and 2; for 200 km it is between 0.5 and 1.5.

For a satellite which is not expected to remain in orbit for more than a fraction of a solar cycle, the density  $\bar{\rho}_p$  in equation (19) needs to be the mean density during the remaining lifetime. This is extremely difficult to estimate, particularly at solar minimum, when it is not known how soon the solar activity will begin to increase. For example, in 1975 it seemed likely that solar activity would increase in 1976; in 1976, a sharp increase early in 1977 seemed almost inevitable. But neither expectation was fulfilled.

The only good thing to be said about the solar-cycle variation is that it loses its importance for satellites with lifetimes of only a few months - and these form the most important group.

#### 4.4.2 Satellites with lifetimes of several solar cycles

If the satellite lifetime exceeds about three solar cycles, the rate of decay is very slow, and it is often difficult to calculate a current value of

in accurately. It is then useful to express  $L$  in terms of the mass/area ratio of the satellite  $m/S$ , assuming a density profile averaged over a solar cycle. This average is taken to be the same as in the past few cycles, the density being taken as that given by the CIRA 1972 model with exospheric temperature 900 K: this density is slightly higher than that given by the mean curve in Fig 13. It should be emphasized, however, that the average density in the future may differ greatly from this value, particularly if in the next 50 years there is a period of low solar activity akin to the 'Maunder minimum' which occurred between 1640 and 1710, when sunspots were a rarity<sup>16,17</sup>.

An equation for  $L(S/m)$  as a function of perigee density  $\rho_p$  and eccentricity may be found from equation (7.6) of Ref 11, namely

$$\rho_p = - \frac{\dot{T}\Sigma(e)}{\delta\sqrt{aH}} , \quad (20)$$

where  $\Sigma(e)$  is a function of  $e$  given in Fig 7.1 of Ref 11. In equation (20) the rate of change of period  $\dot{T}$  (days/day) may be written as  $-\dot{n}/n^2$ ; also  $\delta = FSC_D/m$ , where the drag coefficient  $C_D$  will for the moment be taken as 2.2, and  $F$  is a factor which may be taken as  $0.91 \pm 0.05$  for  $0 < i < 75^\circ$  (the error is larger for  $i > 75^\circ$ , but still much smaller than the possible errors in the assumed future density values). Thus equation (20) becomes

$$\rho_p \sqrt{H} \left( \frac{2n^2 \sqrt{a}}{\Sigma(e)} \right) = \dot{n} \left( \frac{m}{S} \right) , \quad (21)$$

where  $n$  is in rev/day,  $\dot{n}$  in rev/day<sup>2</sup>,  $m$  in kg,  $S$  in m<sup>2</sup>,  $H$  and  $a$  in m, and  $\rho_p$  in kg/m<sup>3</sup>. Taking  $n = 274.5(10^{-6}a)^{-1.5}$ , and  $10^{-6}a = (6.37 + 10^{-3}y_p)/(1 - e)$ , where  $y_p$  is the perigee height in km, equation (21) may be rewritten as

$$G(y_p) \Sigma(e) = \dot{n} \left( \frac{m}{S} \right) , \quad (22)$$

$$\text{where } G(y_p) = 10^6 \rho_p \sqrt{H} \left( 1 + \frac{y_p - 200}{6570} \right)^{-2.5} \quad (23)$$

$$\text{and } \Sigma(e) = 1.362(1 - e)^{2.5} / \Sigma(e) . \quad (24)*$$

---

\* Although  $\Sigma(e)$  depends primarily on  $e$ , it is also dependent on  $H$  when  $e$  is small. When  $e < 0.02$ , we may write  $\Sigma(e)$  as

$$12.84(a/H)^{\frac{1}{2}} \exp(-z) I_0(z) \{1 - e(2.5 - 2I_1/I_0)\} .$$

When  $e = 0.02$ , the variation of  $\Sigma(e)$  is about  $\pm 4\%$ . Values of  $\Sigma(e)$  for  $e > 0.2$  are shown in Fig 21.

From equations (22) and (9) we have

$$L(S/m) = Q/\{365G(y_p)\Sigma(e)\} \quad (25)$$

if  $L$  is to be in years rather than days.

Fig 14 shows the values of  $L(S/m)$  given by equation (25) for perigee heights of 200-2000 km, and eccentricities between 0 and 0.8. The values of  $Q$  ( $= L\dot{n}$ ) are obtained from equations (5), (6) or (8).  $G(y_p)$  is obtained from equation (23) and *CIRA 1972*, and  $\Sigma(e)$  from equation (24) and Fig 7.1 of Ref 11. The density profile in *CIRA 1972* leads to some wide excursions in the values of  $\mu$  at heights between 750 and 1000 km, which lead to corresponding excursions in the curves for  $L$ : these have been smoothed out in drawing the curves in Fig 14, to assist in interpolation. It should be emphasized again (a) that the curves of Fig 14 are subject to considerable uncertainty, because the future level of solar activity in the next 50 to 100 years is not known, and (b) that the results only apply when the satellite experiences an average density corresponding to that given in *CIRA 1972* for an exospheric temperature of 900 K - the average over recent solar cycles. This means that, in general, the curves of Fig 14 should only be used if the satellite is in orbit for at least three solar cycles, or approximately 30 years. However, the curves can sometimes give a good indication of shorter lifetimes: if a satellite is launched at solar minimum, and Fig 14 indicates a lifetime of 5 years or 11 years, these values might be quite accurate if it turns out that the 5 years are from minimum to maximum of a typical solar cycle, or the 11 years make up a complete and fairly average solar cycle. In these special circumstances, the density experienced by the satellite will be 'average'. A diagram similar to Fig 14 has been given by Perini<sup>18</sup>.

To obtain the lifetime in years, the values of  $L(S/m)$  in Fig 14 must be multiplied by the mass/area ratio of the satellite,  $m/S$ , expressed in  $\text{kg/m}^2$ . The value of  $S$  is the average cross-sectional area, equal to  $\frac{1}{4}\pi d^2$  for a sphere of diameter  $d$ , and approximately equal to  $0.8\ell d$  for a tumbling cylinder of length  $\ell$  and diameter  $d$ . The numerical value of  $m/S$  is often near  $100 \text{ kg/m}^2$ , and the values of  $L$  in Fig 14 would then lie between 10 years and  $10^6$  years. Values of  $m/S$  for a variety of satellites are given in Fig 15: the values are between 50 and 200  $\text{kg/m}^2$  for nearly all satellites.

When the perigee height exceeds 600 km, the drag coefficient assumed here, 2.2, is likely to increase<sup>19</sup>, possibly to values as high as 3, because of the decrease in the ratio of satellite velocity to molecular velocity. No allowance

has been made here for this increase, because its exact form is not known; if  $C_D$  is known to differ from 2.2, the lifetime  $L$  should be multiplied by  $2.2/C_D$ .

The results presented in this section are of course not strictly 'corrections' to the previous methods, but rather an alternative method, when the usual  $\dot{n}$ -method becomes impracticable, because the current value of  $\dot{n}$  cannot be accurately estimated.

#### 4.4.3 The day-to-night variation

The day-to-night variation in air density is not so large as the solar-cycle variation, as Fig 13 shows. But the maximum daytime density can exceed the minimum night-time density by a factor of up to 5 at 500 km height, so that a lifetime calculated from the value of  $\dot{n}$  when the perigee density is at the night-time minimum can be in error by a factor of 3 if the perigee later experiences the average density. If, as is more usual, the perigee height is between 200 and 250 km, the error factor is less, though still important - having a maximum value near 1.5. Usually perigee goes through a day-to-night cycle in a few months. As with the solar-cycle variation, the remedy is to adjust the lifetime by multiplying by  $\rho_p/\bar{\rho}_p$  where  $\rho_p$  is the current density at perigee and  $\bar{\rho}_p$  the mean value over the remaining lifetime, which would be the mean value over a day-to-night cycle if perigee is to sample several such cycles.

The day-to-night variation is somewhat intractable, because even the current local time at perigee is not readily available and needs to be calculated; its future variation is not accurately predictable, because it depends on the rate of decay, which itself depends on the variation of local time. For satellites of several years life, the best policy is to calculate  $\dot{n}$  at a time when the density at perigee is near the mean of the day-to-night variation, that is, when the local time at perigee is near 09h or 20h local time.

The only helpful feature of the day-to-night variation is that it becomes small as decay approaches: for a perigee height of 250 km the maximum value of  $\rho_p/\bar{\rho}_p$  (for low solar activity) is 1.4, decreasing to 1.2 at 200 km. When solar activity is high, the corresponding values are 1.2 and 1.1. Also, when the satellite is within a month or two of decay, the mean value of  $\rho_p$  during the remaining life is likely to be nearer to the current value than to the mean value over a complete day-to-night cycle.

#### 4.4.4 The semi-annual variation

In addition to the wide variations shown in Fig 13, the air density undergoes a fairly regular semi-annual variation with maxima usually in April and October, and minima usually in January and July. Although the variations are smaller in amplitude than the solar-cycle and diurnal effects - the factor of variation is about 1.6 at heights near 200 km, increasing to about 3 at 500 km - the semi-annual variation is more important for lifetime estimation (a) because it extends down to 150 km height without much diminution, and (b) because the 3-month interval between maximum and minimum introduces considerable errors into the most important lifetime estimates, those of between 2 and 6 months.

The semi-annual effect varies from year to year in amplitude and phase, and cannot yet be predicted accurately. A standard variation is given in *CIRA*, but this has proved to be inadequate in the 1970s, and it is preferable to use the variation of density recommended by Walker<sup>20</sup>, shown in Fig 16. These values,  $V$ , are based on results in 1972-5 at heights of 200-250 km, which is the most likely range of perigee heights for satellites with lifetimes of a few months.

To allow for the semi-annual variation, the lifetime  $L$  should be multiplied by  $V/\bar{V}$ , where  $V$  is the value at the current date, and  $\bar{V}$  is the mean value of  $V$  during the remaining lifetime. Again, an iterative procedure may be needed if  $V/\bar{V}$  differs greatly from 1.

In Fig 17 the semi-annual correction  $V/\bar{V}$  is plotted against lifetime, for lifetimes of up to 160 days, for predictions made on particular days of the year - year days 0, 20, 40, 60 ... 340. The correction for intermediate dates can be found by interpolation. Although subject to some uncertainty because of the yearly variations in the amplitude and phase of the semi-annual variation, Fig 17 provides an easy and reasonably accurate correction, which needs to be used for all lifetime estimates of less than 160 days.

Fig 18 shows the variation of  $V/\bar{V}$  during the course of the year for satellites with lifetimes of (a) 20-100 days and (b) 100 days to 1 year.

For satellites with lifetimes of many years, errors due to the semi-annual variation may be minimized by taking values of  $\bar{V}$  calculated near the mean of the semi-annual variation, that is, near 19 February, 14 May, 17 September or 30 December, where  $V/\bar{V} = 1$ .

#### 4.4.5 Irregular day-to-day variations

Air density at heights above 150 km suffers continual day-to-day variations of order  $\pm 10\%$ , and much larger variations (by a factor of up to 2 at 200 km and 6 at 600 km) at times of major geomagnetic disturbances. These irregular day-to-day effects must be regarded as largely unpredictable at present, although some of the likely variations may be partially predictable from the 27-day recurrence tendency in solar activity: forecasts of solar activity and geomagnetic disturbances up to 3 days ahead are made daily by the USAF Geophysical Warning Center. The skilled predictor will take advantage of any available information of this kind, which can be most useful for decay predictions at the very end of a satellite's life. The possibility of unexpected magnetic storms remains, however, and predicted lifetimes of about 4 days may prove to be too large by a factor of 2 if a major geomagnetic storm occurs on the day after the prediction is made.

In predicting decays several months ahead, future day-to-day variations are less important; but the *current* rate of orbital decay may be calculated at an extreme of the current day-to-day irregularities. To avoid this danger, it is usually better to evaluate the current rate of decay over at least 2 or 3 days. A subtler stratagem, for an important decay, is to make predictions every day or two and to take a weighted mean value, with weighting inversely proportional to the remaining lifetime, as proposed in Ref 31.

#### 4.5 Envoi

After hearing of all these corrections, so many of them intractable or unpredictable, anyone who contemplates making predictions may well feel like giving up in despair and may seek refuge in elaborate computer programs of numerical integration. This apparent escape route, discussed in section 5, is partly illusory, because the solar activity and semi-annual corrections still have to be specified separately, and the peril of the unpredicted geomagnetic storm still lurks around.

Despite the difficulties of making all the corrections, the graphical methods do often yield lifetime estimates accurate to about 10%, though much larger errors can easily be made if a necessary correction is neglected.

### 5 PROCEDURES WHEN LUNISOLAR PERTURBATIONS ARE LARGE

#### 5.1 The PROD program

If the perigee height suffers large perturbations due to lunisolar gravitational attraction, the approximate analytical methods described in sections 2 to 4

become ineffective, and it is necessary to resort to numerical integration. For this purpose the computer program PROD (program for orbital development) was developed by G.E. Cook<sup>21</sup> in the 1960s. To avoid excessive use of computer time, the effects of solar radiation pressure and air drag are omitted in PROD and the lunisolar disturbing functions are averaged analytically with respect to the mean anomaly of the satellite. Zonal harmonics in the geopotential and harmonics in the expansion of the solar and lunar potential up to the ninth can be included, although in practice only the second harmonic of the solar potential and up to the third in the lunar are required. The interval of integration can be chosen by the user.

PROD has been applied in a large number of long-term lifetime predictions. It has been particularly valuable in predicting the lifetimes of Molniya satellites with eccentricities near 0.7 initially. The usual effect of lunisolar perturbations on these satellites, and on many rockets left in transfer orbits with low perigee, high apogee and eccentricity near 0.7, is to produce an oscillation in perigee height with an amplitude of several hundred kilometres and a period of several years. PROD allows the forward integration of the orbit for many years, and the date when the perigee is driven down to a height near 100 km usually indicates the likely decay date to within a few months. In quoting lifetimes, we usually add about 30 days to the value given by PROD, to allow for a short period of decay under air drag, which is often found to occur in practice. For satellites of long life, an integration interval of 20 days is often used with PROD, to save computer time: comparison with computations having integration intervals of 10 days and 5 days usually shows no great differences. Shorter intervals, down to 1 day, are used when more detailed results are required. Many examples of orbital evolution calculated by means of PROD have been given<sup>22-24</sup>, and one is reprinted as Fig 19.

There are two main difficulties in predicting the evolution of these high-eccentricity orbits using PROD. The first problem is the neglect of drag in the program, and this is discussed in section 5.3. The second problem is the inevitable inaccuracy of the initial values of perigee height used in the computation. The USAF NORAD elements are nearly always the only elements available for these satellites, and since the satellites are very difficult to track, often being at great heights in the northern hemisphere, the orbits are often based on inadequate numbers of observations poorly distributed round the orbit, so that bias errors in eccentricity arise, and errors of up to 30 km or even 50 km in perigee height are not uncommon. If the perigee height decreases slowly from 200 km to 100 km at the end of the life, such absolute errors in initial perigee

height, which tend to be carried through the integration, can obviously cause serious errors in the estimates of decay date.

Despite these limitations, PROD is often successful in adverse circumstances. Fig 20 shows a particularly unfavourable recent example, the satellite 1972-37A, predicted from an initial orbit in March 1973. The initial orbit was probably not very accurate, and the integration interval was rather too great for good accuracy (25 days); also the perigee dipped low into the atmosphere in November 1973, and decay might have occurred then, but did not. Yet the decay date predicted by PROD in 1973, with the 30-day addition mentioned earlier, was 21 March 1977: the actual decay date was 22 March 1977. Fig 20 also shows the perigee height, calculated from the decay rate  $\dot{n}$  in NORAD bulletins, as described in section 5.2, for the occasions when  $\dot{n}$  is large enough to be reliable.

### 5.2 Calculation of perigee height from decay rate

The normal method of calculating perigee height, from the value of  $a(1-e)$ , is, as already mentioned, subject to errors of 30 or 50 km for high-eccentricity orbits. If the perigee height is near 200 km, a change of 30 km in perigee height changes the air density at perigee and hence the decay rate by a factor of about 3. Such errors in perigee height are obviously unacceptable if accurate forecasts of lifetime are to be made, and the sensitivity of  $\dot{n}$  to perigee height means that a better estimate of perigee height can often be obtained from  $\dot{n}$  if the mass/area ratio  $m/S$  of the satellite is known. If  $m/S$  and  $\dot{n}$  are both known accurate to about  $\pm 10\%$ , an accuracy of  $\pm 5$  km in perigee height can be achieved for heights near 200 km, or an accuracy of  $\pm 3$  km if perigee height is near 150 km.

The relation between  $\dot{n}$  and  $\rho_p$  may be found from equation (22), and since we may assume that the perigee height is  $200 \pm 70$  km, equation (23) gives  $G(y_p) = 10^6 \rho_p \sqrt{H}$ , whence

$$\dot{n} \left( \frac{m}{S} \right) = 10^6 \rho_p \sqrt{H} \Sigma(e) \quad (26)$$

Fig 21 gives values of  $\Sigma(e)$  for  $e > 0.2$ , and Fig 22 gives values of  $10^6 \rho_p \sqrt{H}$  from CIRA 1972 for  $100 < y_p < 260$  km, for low and high solar activity (exospheric temperature 800 and 1100 K).

Fig 23 shows the variation of  $\dot{n}(m/S)$  with  $y_p$  for selected values of  $e$  close to those most often used: for example, many satellites (including the Molniyas) have eccentricities between 0.7 and 0.75 during nearly the whole

lifetime, and curves are given for these two values but not for  $e = 0.6$ , a value which rarely arises.

To use Fig 23, the value of  $\dot{n}$  (rev/day<sup>2</sup>) is calculated from the two latest USAF bulletins available (or, less accurately, from the value of  $\dot{n}/2$  given on the latest bulletin), and multiplied by  $m/S$ . The corresponding value of  $y_p$  is then read from Fig 23, for the appropriate values of  $e$  and solar activity. An alternative and more accurate method is to use equation (26) directly:  $\dot{n}(m/S)$  is calculated as before and divided by  $\Sigma(e)$ , from Fig 21, to give a value of  $10^6 \rho_p \sqrt{H}$  and hence  $y_p$  from Fig 22.

If we assume that the value of  $y_p$  derived from  $\dot{n}$  is correct and call it  $y_{pn}$ , and if the initial value of  $y_p$  in a PROD run derived from  $a(1 - e)$  is  $y_{pe}$ , then PROD should be re-run with  $e$  adjusted to give the correct perigee height; that is,  $e$  should be increased by  $\Delta y_p/a$ , where  $\Delta y_p = y_{pe} - y_{pn}$ .

### 5.3 The PTDEC program

The program PTDEC, which allows for drag as well as lunisolar perturbations, has recently been developed by Palmer<sup>25</sup>, as a shortened version of the program POINT<sup>26</sup> (program for orbit integration). The name PTDEC may be regarded as an acronym for POINT to decay. The integration step in PTDEC is normally 1/96 of a revolution, and the reference atmosphere used is a simplified version of the Jacchia 1965 model<sup>27</sup>, a precursor of CIRA 1972. The integration ends when the perigee height drops to 90 km (or any specified greater value). Values of  $S/m$  and solar 10.7 cm radiation energy have to be supplied by the user, and these values are kept constant during the computer run.

PTDEC needs much more computer time than PROD, and is essentially a method for use in the last few months of a satellite's life. The main difficulty is again the inaccuracy in the initial perigee height, and it is usually necessary to have a 'trial run' first, with  $e$  somewhat reduced to avoid the possibility of an initial perigee height lower than 90 km, and then a re-run with a corrected value of  $e$ , as described in section 5.2.

Fig 24 shows the variation of apogee and perigee height as given by PTDEC for the last two months in the life of 1972-37A, a typical rapid-decaying satellite. In this example the orbit was being re-run with the perigee height given by PTDEC arranged to coincide with the perigee height deduced from the value of  $\dot{n}$  in NORAD bulletin 329, namely 207 km; values of perigee height

obtained from other NORAD bulletins are shown as circles. The lifetime indicated by PTDEC was 63 days from January 25, a date at which the semi-annual correction  $V/\bar{V}$  is 0.87, from Fig 17. Thus the lifetime given by PTDEC, corrected for the semi-annual variation, is 55 days: the actual lifetime was 56 days, so the agreement is excellent. In running PTDEC, the solar  $F_{10.7}$  index was taken as 80, which proved to be a good approximation to the actual value in February-March 1977, namely 79. The value of  $S/m$  was taken as  $0.01 \text{ m}^2/\text{kg}$  in PTDEC, and it may seem surprising that such an accurate lifetime estimate was obtained, using such a 'round-number' value of  $S/m$ : but since the perigee height is obtained from  $\dot{n}$  assuming this *same* value of  $S/m$ , the initial decay rate on PTDEC should be the same as on the actual orbit, even if  $S/m$  is in error, and the effects of errors in the value of  $S/m$  are much less than might be expected.

Fig 24 is also of interest in its own right, as an example of very rapid decay. Most of the decrease in perigee height during February is due to luni-solar perturbations: the decrease due to drag, approximately  $\frac{1}{2}H \ln(e_0/e)$ , is less than 80 m (with  $e_0 = 0.750$  and  $e = 0.743$  on 5 March). The decrease in perigee height due to drag only becomes appreciable in the last 10 days of the life. The apogee height indicated by PTDEC in Fig 24 decreases fairly steadily during the week before decay at the extremely rapid rate of 3000 km per day. The maximum daily decrease is 3500 km, two days before decay.

PTDEC can, of course, also be used for orbits of low eccentricity, and it has the advantage over the graphical methods that it automatically takes account of the variations in perigee height discussed in section 4.2. However, PTDEC does not allow for the day-to-night or semi-annual variations in density, or the future variations of solar activity; so these still have to be estimated separately. For low-eccentricity orbits the value of perigee height from NORAD elements, with the appropriate corrections<sup>28</sup>, should be accurate to 2 km, so there is no need to obtain perigee height from  $\dot{n}$ . Instead it is possible to use  $\dot{n}$  to determine  $S/m$  for use in the program if, as often happens, the value of  $S/m$  is not known. The procedure is to guess  $S/m$  for a first run, and then to adjust it so that the initial value of  $\dot{n}$  given by PTDEC is the same as that of the actual satellite. The values of  $m/S$  for a representative selection of actual satellites are shown in Fig 15. Values of  $m/S$  near  $100 \text{ kg/m}^2$  are common, and  $0.01 \text{ m}^2/\text{kg}$  is an appropriate value to use as a first guess in the PTDEC run.

#### 5.4 Decrease in drag coefficient at low altitudes

The theory so far used here has relied on the assumption that the drag coefficient  $C_D$  of the decaying satellite remains constant, and when a numerical value is needed, as in equation (20),  $C_D$  has been taken as 2.2. This is the value appropriate<sup>19</sup> in free-molecule flow, when the mean free path of the molecules greatly exceeds the dimensions of the satellite. When the mean free path becomes comparable to the dimensions of the satellite, however, the drag coefficient decreases to about half its value in free-molecule flow<sup>29</sup>. The mean free path (Fig 25) decreases from 10 m at 130 km height to 3 m at 120 km height: so, for all satellites except the smallest, the remaining lifetime after perigee has descended to 120 km is likely to be double that expected on the basis of a constant value of  $C_D$ . For low-eccentricity orbits, this effect is usually negligible in predicting decay dates weeks or months ahead, because perigee does not drop below 120 km until within a few revolutions of decay. The effect is also negligible for high-eccentricity orbits, if the perigee height is being driven down by lunisolar perturbations. For some high-eccentricity orbits, however, the lunisolar perturbations can, on occasions when they are tending to push the perigee height upwards, combat and sometimes outdo the decrease in perigee height due to air drag. When this happens, the satellite can be kept in orbit for days or even weeks with perigee below 120 km. An example is 1970-114F, where the perigee height was below 113 km during the last 20 days of the life<sup>30</sup>, and the drag coefficient was calculated to be  $0.85 \pm 0.20$ .

The general effect of the decrease in  $C_D$  when the mean free path decreases to a value comparable to the dimensions of the satellite, is shown in Fig 26, which gives lifetimes for satellites of length 10 m (unbroken lines) and 1 m (broken lines), for  $m/S = 100 \text{ kg/m}^2$ . The lifetime is proportional to  $m/S$ , in the absence of strong lunisolar perturbations. From Fig 26 it is obvious that the change in  $C_D$  has a large relative effect; but most satellites have eccentricities less than 0.01 by the time perigee height has decreased to 130 km, so the change in lifetime for these satellites is less than 0.2 day (for  $m/S = 100 \text{ kg/m}^2$ ).

For the few satellites which are affected seriously by the decrease in  $C_D$ , the easiest way of allowing for it is to double the remaining lifetime given by PTDEC after the time,  $t^*$  say, when the perigee first descends to the height where the mean free path equals the length of the satellite. A more accurate procedure, necessary when lunisolar perturbations are still strong

(if  $e > 0.5$ ), is to re-run PTDEC from time  $t^*$  onwards with the original value of  $S/m$  halved: this is equivalent to reducing  $C_D$  to half its value in free-molecule flow.

## 6 CONCLUDING REMARKS

The aim of this paper has been to outline the many problems encountered in satellite decay predictions, and to provide solutions to as many as possible - but regrettably not all.

To summarize, the lifetime  $L$  of satellites in orbits of eccentricities between 0 and 0.8 is written as  $Q/n$ , where  $n$  is the current decay rate, and values of  $Q$  are given first in Fig 2, and then more accurately in Figs 5, 6, 8 and 10, for an idealized spherically symmetrical Earth and atmosphere. Corrections to these values for the effects of variations in perigee height and semi-annual density variations are shown in Figs 11-12 and 17-18 respectively, and other corrections are discussed in section 4. For orbits which suffer serious lunisolar perturbations, numerical-integration methods are needed, and the use of these is described in section 5.

For the majority of non-manoeuvring satellites, these methods allow the prediction of decay dates up to about one year ahead with an accuracy of about 10% of the remaining lifetime, if sufficient care is taken. But the lifetime depends on a multiplicity of independent variables, including the rotational behaviour of the satellite (which affects the cross-sectional area), the time variations of the atmosphere (particularly the semi-annual variation), the future variations in solar activity (for which prediction is poor at present), the gravitational fields of the Earth, Sun and Moon (whose effects on the orbit themselves depend on the future evolution of the orbit), and the future values of the local time and latitude at perigee (which depend on most of the factors previously mentioned). Further difficulties are that current orbital elements may not be available, or that the available elements are inaccurate. For a small minority of satellites one or more of these difficulties arises in acute form, and can greatly degrade the accuracy of the lifetime estimates.

REFERENCES

<u>No.</u>	<u>Author</u>	<u>Title, etc</u>
1	D.M.C. Walker	Table of artificial satellites, January 1961. RAE Technical Memorandum GW 386 (1961) [Also <i>Discovery</i> , <u>22</u> , 220, May 1961]
2	D.G. King-Hele H. Hiller J.A. Pilkington	Table of Earth satellites, Vol 1: 1957 to 1968 RAE Technical Report 70020 (1970)
3	J.A. Pilkington D.G. King-Hele H. Hiller	Table of Earth satellites, Vol 2: 1969 to 1973 RAE Technical Report 74105 (1974) Also Vol 3, Parts 1-3: 1974-1976 (to be issued as Vol 3, 1974 to 1977, in RAE Technical Report form in 1978)
4	D.G. King-Hele D.C.M. Leslie	Effect of air drag on the orbit of the Russian earth satellite 1957B: comparison of theory and observation. <i>Nature</i> , <u>181</u> , 1761-1763 (1958)
5	G.E. Cook D.G. King-Hele D.M.C. Walker	The contraction of satellite orbits under the influence of air drag. I: with spherically symmetrical atmosphere. <i>Proc. Roy. Soc. A</i> , <u>257</u> , 224-249 (1960) RAE Technical Note GW 533 (1959)
6	G.E. Cook D.G. King-Hele D.M.C. Walker	The contraction of satellite orbits under the influence of air drag. II: with oblate atmosphere. <i>Proc. Roy. Soc. A</i> , <u>264</u> , 88-121 (1961) RAE Technical Note GW 565 (1960)
7	D.G. King-Hele	The contraction of satellite orbits under the influence of air drag. III: high-eccentricity orbits. <i>Proc. Roy. Soc. A</i> , <u>267</u> , 541-557 (1962) RAE Technical Note Space 1 (1962)
8	D.G. King-Hele	A view of Earth and Air. <i>Phil. Trans. Roy. Soc. A</i> , <u>278</u> , 67-109 (1975) RAE Technical Memorandum Space 212 (1974)

REFERENCES (continued)

<u>No.</u>	<u>Author</u>	<u>Title, etc</u>
9	G.E. Cook D.G. King-Hele	The contraction of satellite orbits under the influence of air drag. IV: with scale height dependent on altitude. <i>Proc. Roy. Soc. A</i> , <u>275</u> , 357-390 (1963) RAE Technical Note Space 18 (1963)
10	-	<i>CIRA 1972</i> (Cospar International Reference Atmosphere 1972). Berlin: Akademie-Verlag (1972)
11	D.G. King-Hele	<i>Theory of satellite orbits in an atmosphere</i> . London: Butterworths (1964)
12	D.G. King-Hele G.E. Cook	Analysis of 27 satellite orbits to determine odd zonal harmonics in the geopotential. <i>Planet. Space Sci.</i> , <u>22</u> , 645-672 (1974) RAE Technical Report 73153 (1973)
13	Y. Kozai	The motion of a close Earth satellite. <i>Astronom. J.</i> , <u>64</u> , 367-377 (1959)
14	G.E. Cook	Lunisolar perturbations of the orbit of an Earth satellite. <i>Geophys. J.</i> , <u>6</u> , 271-291 (1962) RAE Technical Note GW 582 (1961)
15	D.G. King-Hele G.E. Cook D.W. Scott	Odd zonal harmonics in the geopotential, determined from 14 well-distributed satellite orbits. <i>Planet. Space Sci.</i> , <u>15</u> , 741-769 (1967) RAE Technical Report 66317 (1966)
16	E.W. Maunder	A prolonged sunspot minimum. <i>Knowledge</i> , <u>17</u> , 173-176 (1894)
17	J.A. Eddy	The Maunder minimum <i>Science</i> , <u>192</u> , 1189-1202 (1976)
18	L.L. Perini	Orbital lifetime estimates. Johns Hopkins University Applied Physics Laboratory Report ANSP-M-8 (1974) [Also <i>J. Spacecraft</i> , <u>12</u> , 323-4 (1975)]

REFERENCES (continued)

<u>No.</u>	<u>Author</u>	<u>Title, etc</u>
19	G.E. Cook	Satellite drag coefficients. <i>Planet. Space Sci.</i> , <u>13</u> , 929-946 (1965) RAE Technical Report 65005 (1965)
20	D.M.C. Walker	Variations in air density from January 1972 to April 1975 at heights near 200 km. RAE Technical Report 77078 (1977)
21	G.E. Cook	Basic theory for PROD, a program for computing the development of satellite orbits. <i>Celestial Mechanics</i> , <u>7</u> , 301-314 (1973) [Also RAE Technical Report 71007 (1971)]
22	G.E. Cook D.W. Scott	Long-term evolution of medium-distance orbits. RAE Technical Report 65292 (1965)
23	G.E. Cook D.W. Scott	Further studies of the lifetimes of satellites in large-eccentricity orbits. RAE Technical Report 67189 (1967) [Also <i>Planet. Space Sci.</i> , <u>15</u> , 1549-1556 (1967)]
24	D.G. King-Hele	The orbital lifetimes of Molniya satellites. <i>J. Brit. Interplan. Soc.</i> , <u>28</u> , 783-796 (1975) RAE Technical Report 75052 (1975)
25	M.D. Palmer	The computer program PTDEC. RAE Technical Memorandum Space 248 (1977)
26	G.E. Cook M.D. Palmer	The elliptic orbit integration program POINT. RAE Technical Report 76129 (1976)
27	L.G. Jacchia	Static diffusion models of the upper atmosphere with empirical temperature profiles. <i>Smithsonian Cont. to Astrophys.</i> , <u>8</u> , 215-257 (1965)
28	R.H. Gooding	Some comments on SDC orbital elements, with special reference to the satellite Ariel 3. RAE Technical Memorandum Space 138 (1970)

REFERENCES (concluded)

<u>No.</u>	<u>Author</u>	<u>Title, etc</u>
29	K.S. Hadjimichalis	A study of sphere drag in the transition from continuum to free-molecular flow. University of Oxford, Dept of Engineering Science, Report 1073/73 (1973)
30	D.G. King-Hele	Analysis of the orbit of 1970-114F in its last 20 days. <i>Planet Space Sci.</i> , <u>24</u> , 1-16 (1976) RAE Technical Report 75088 (1975)
31	P.W. Blum W. Priester K. Schuchardt C. Wulf-Mathies	On the decay of satellite orbits. <i>Space Research XVI</i> , pp 197-201 Akademie Verlag, Berlin (1977)

Fig 1

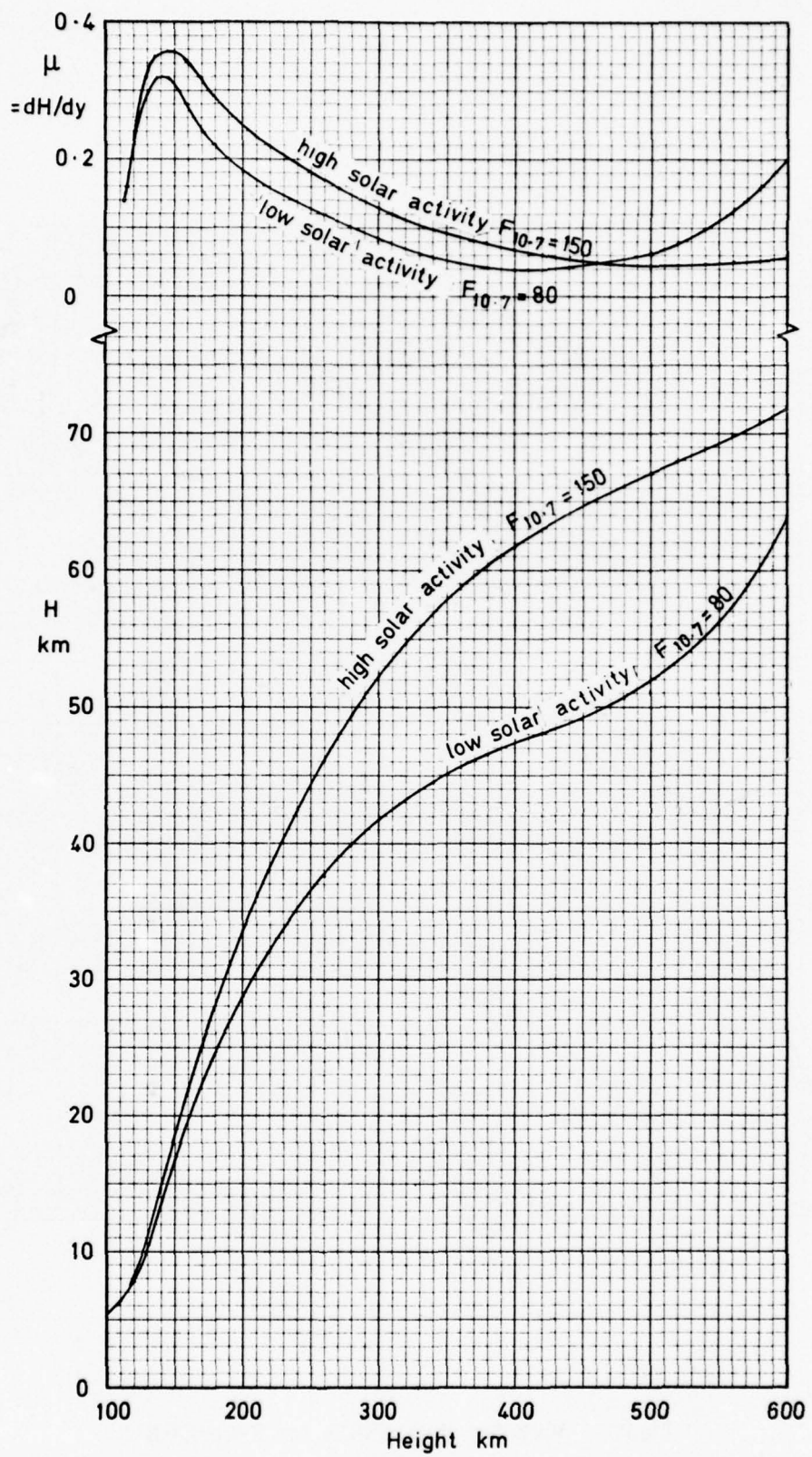


Fig 1 The variation with height  $y$  of density scale height  $H$  and its gradient  $\mu = dH/dy$  as given by CIRA 1972, for high and low solar activity

Fig 2

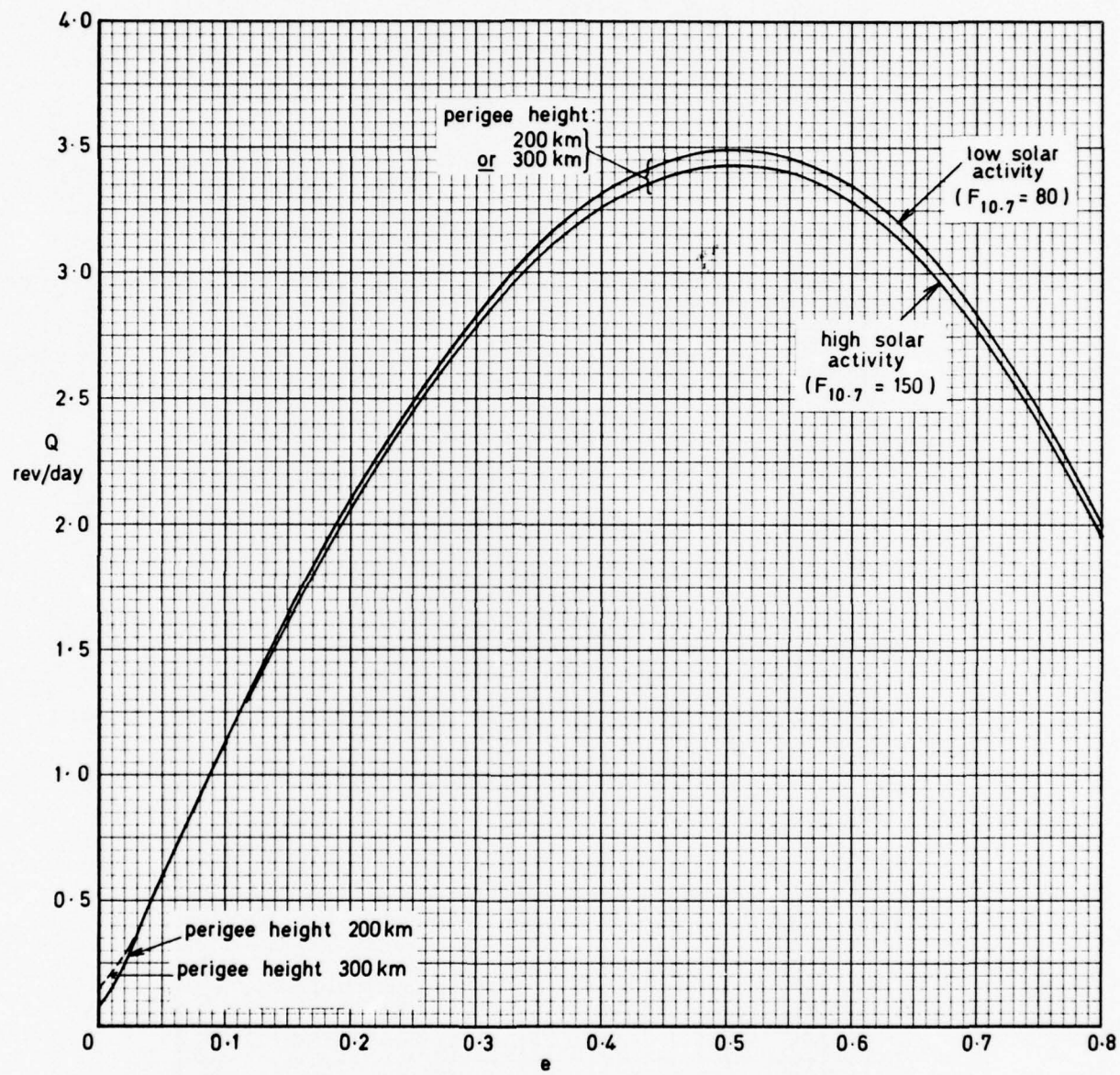


Fig 2 Variation of  $Q$  with  $e$  for  $0 \leq e \leq 0.8$

Fig 3

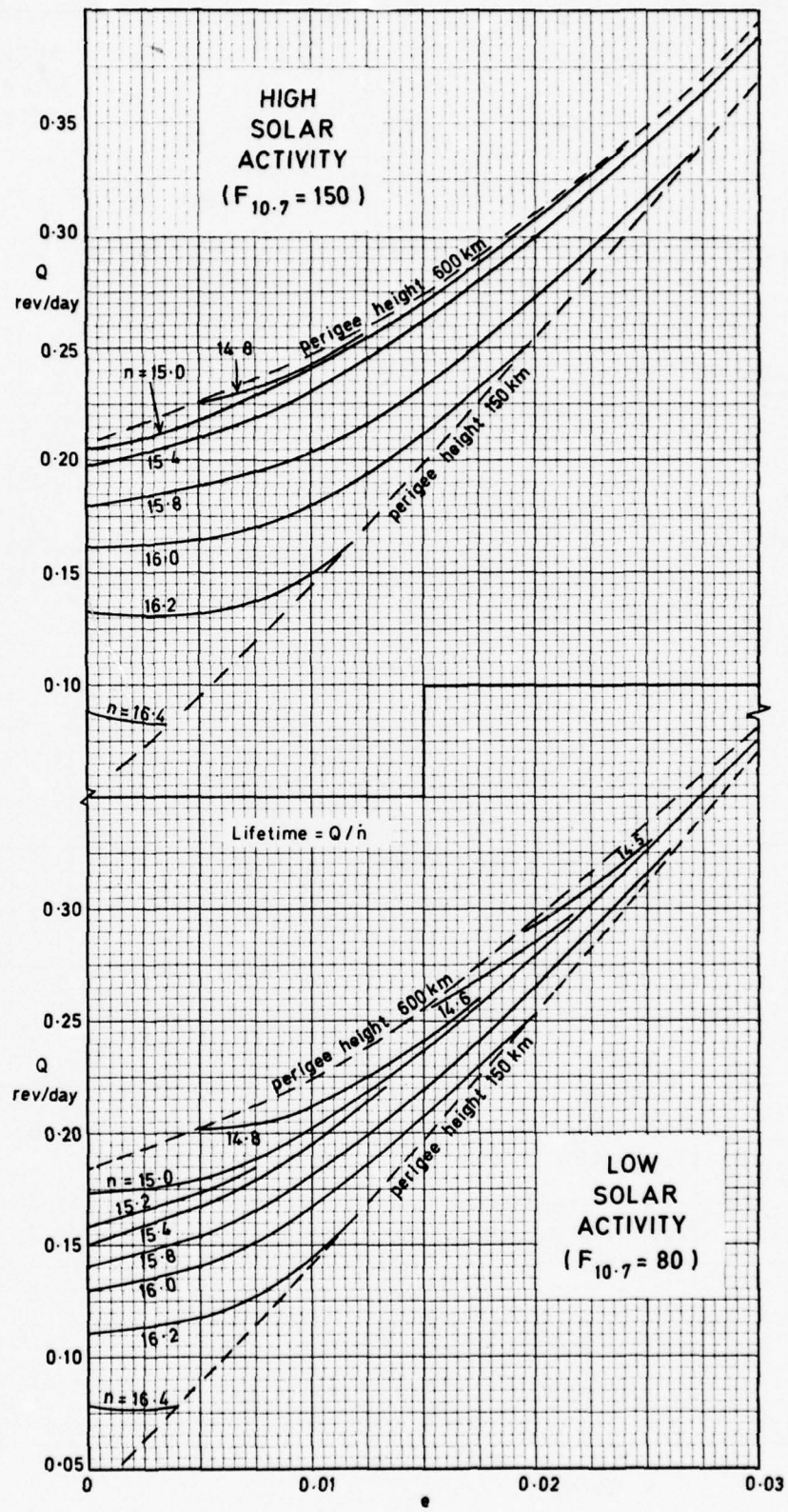


Fig 3 Variation of  $Q$  with  $e$  for  $e \leq 0.03$ , when  $\mu = 0.1$

Fig 4

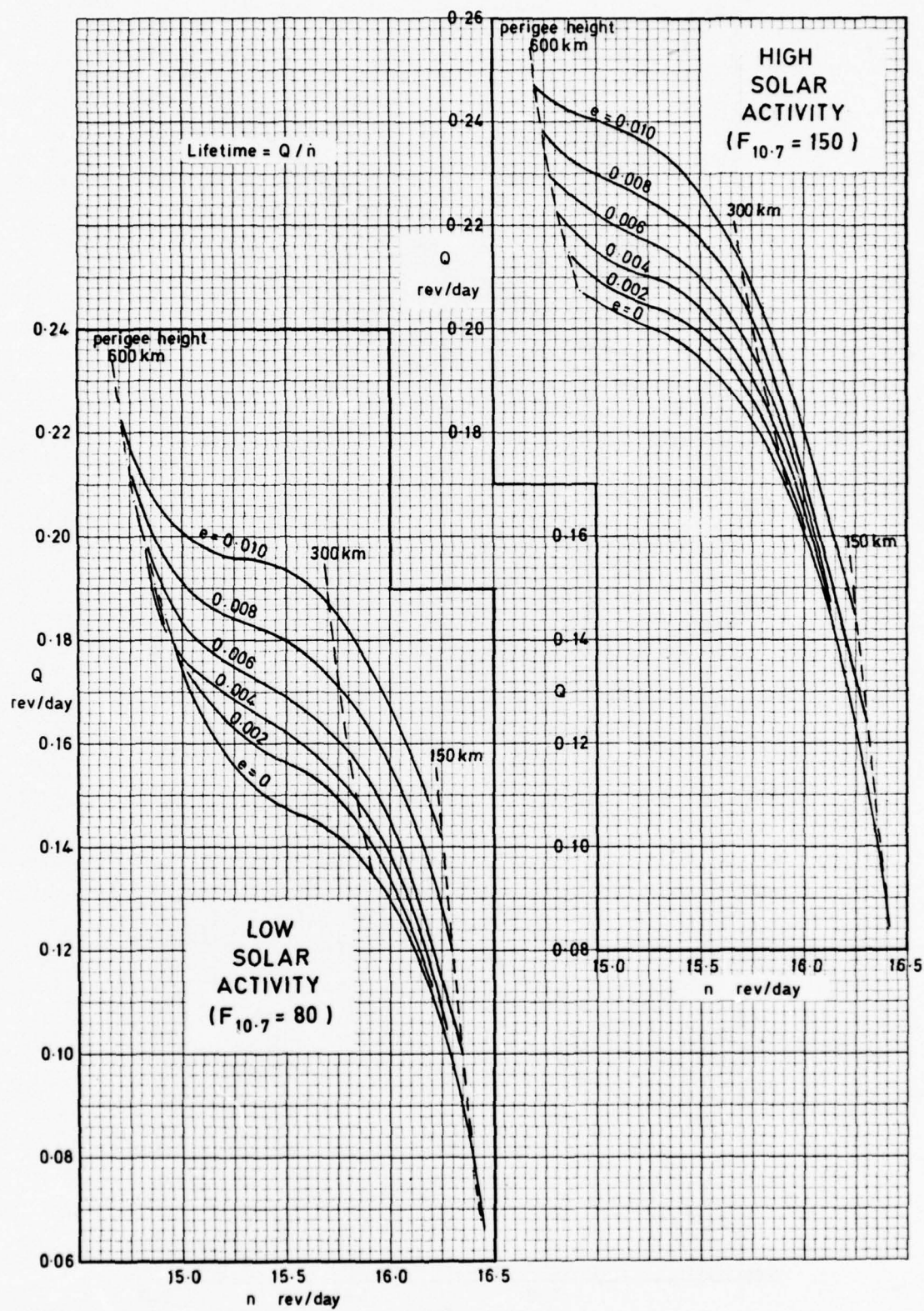


Fig 4 Variation of  $Q$  with  $n$  for  $e \leq 0.01$ , with  $\mu = 0.1$

Fig 5

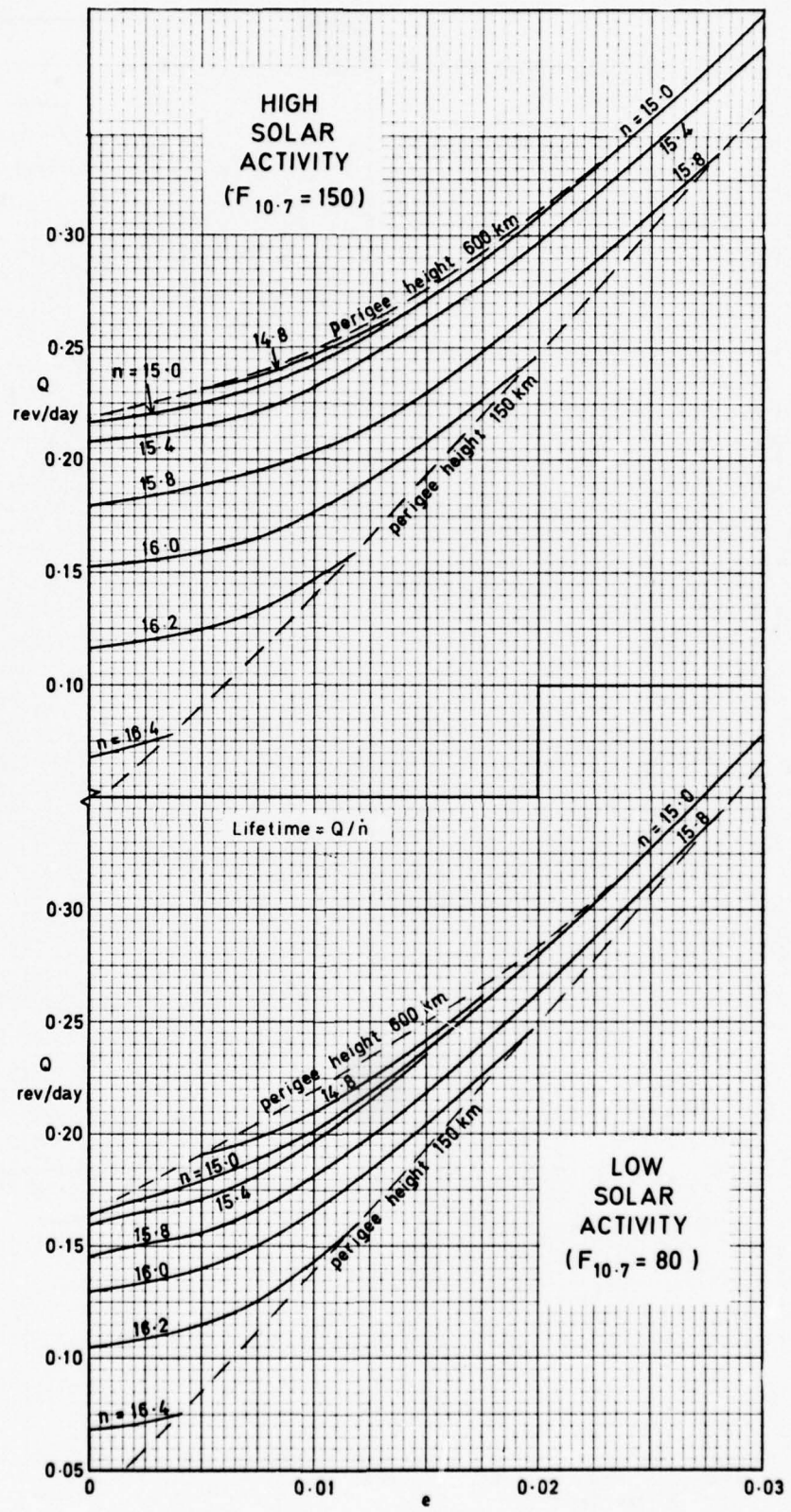
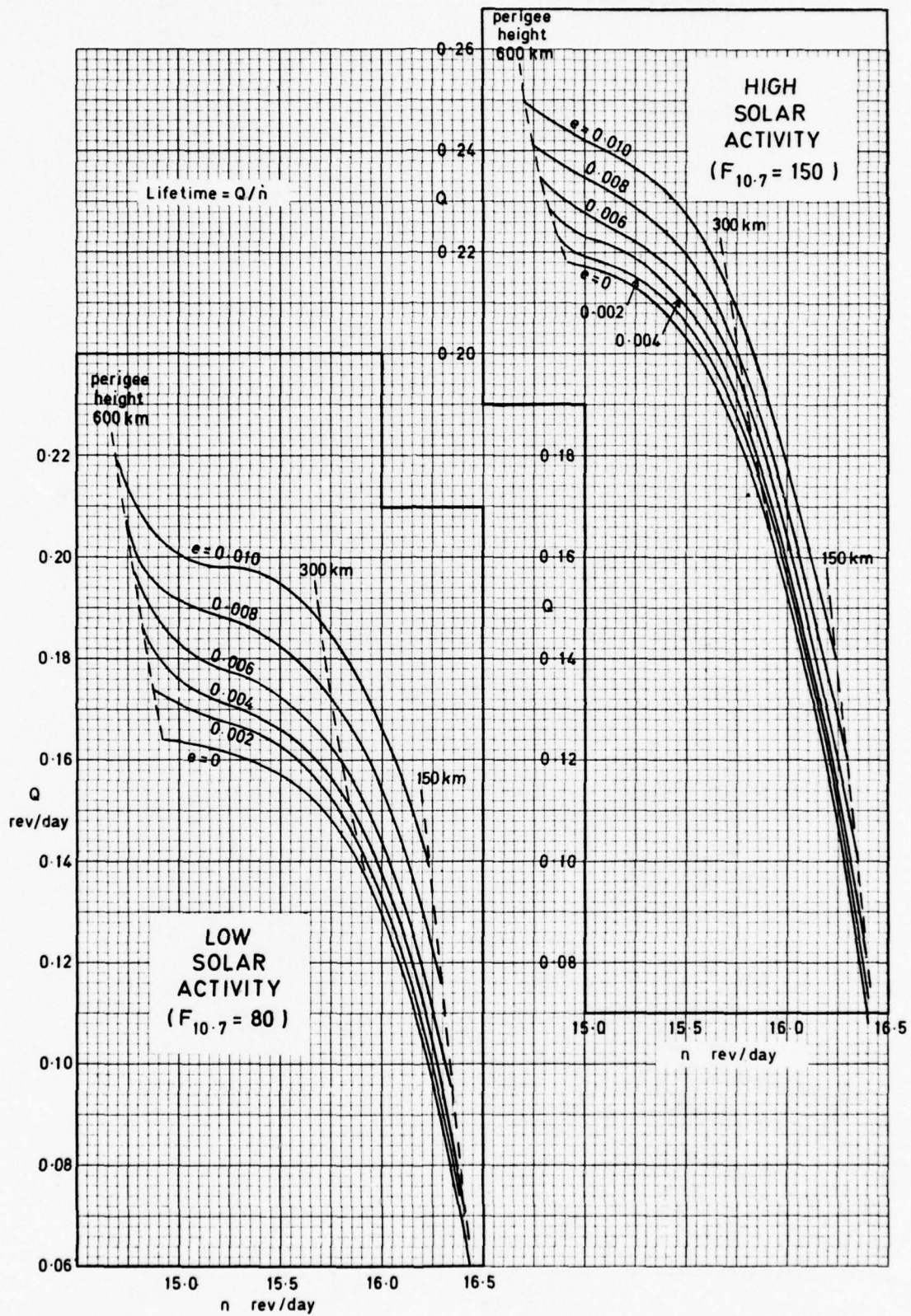


Fig 5 Variation of  $Q$  with  $e$  for  $e \leq 0.03$ , with  $\mu$  from Fig 1

Fig 6



**Fig 6** Variation of  $Q$  with  $n$  for  $e \leq 0.01$ , with  $\mu$  from Fig 1

Fig 7

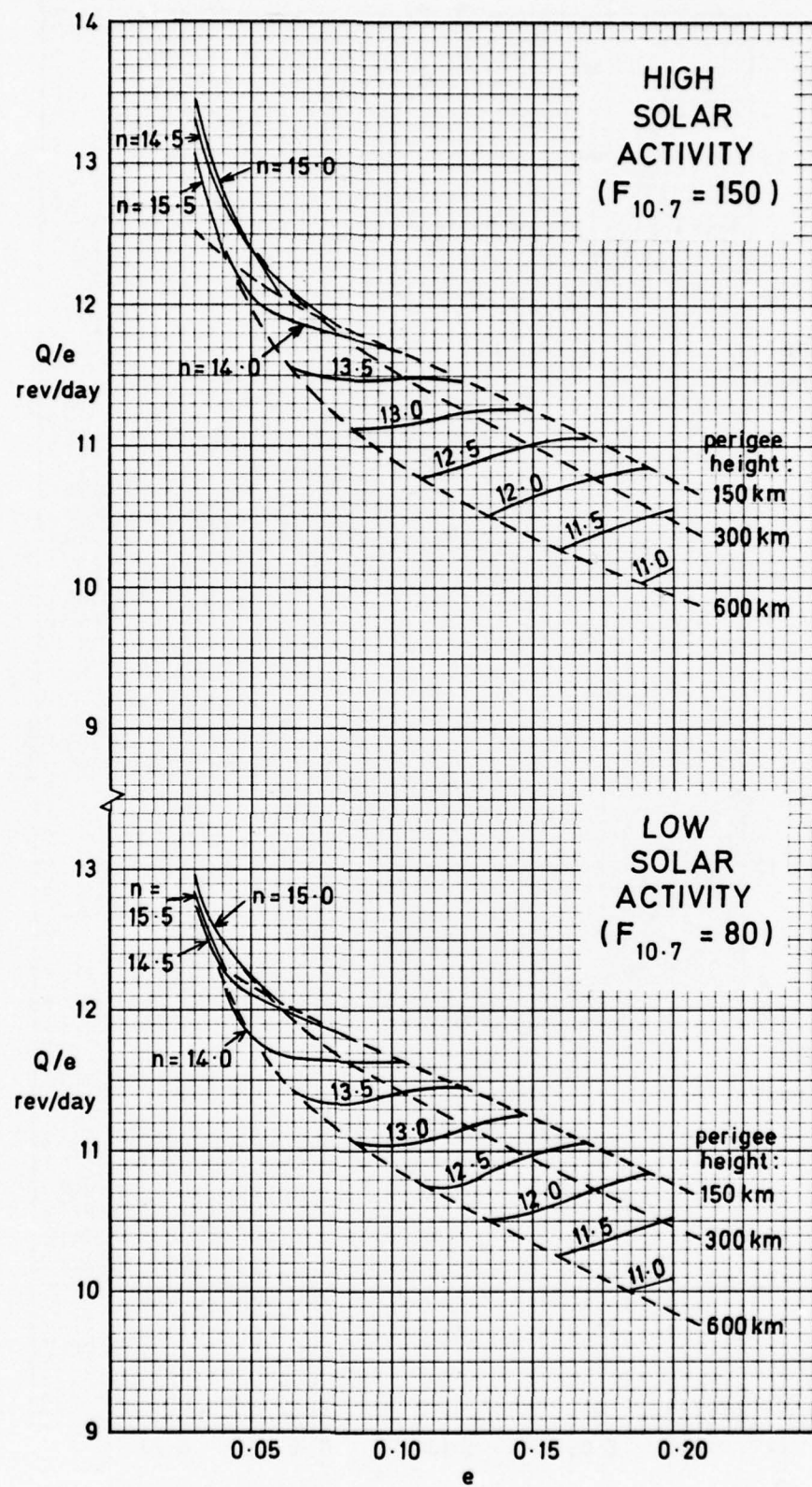


Fig 7 Variation of  $Q/e$  with  $e$  for  $0.03 \leq e \leq 0.2$ , with  $\mu = 0.1$

Fig 8

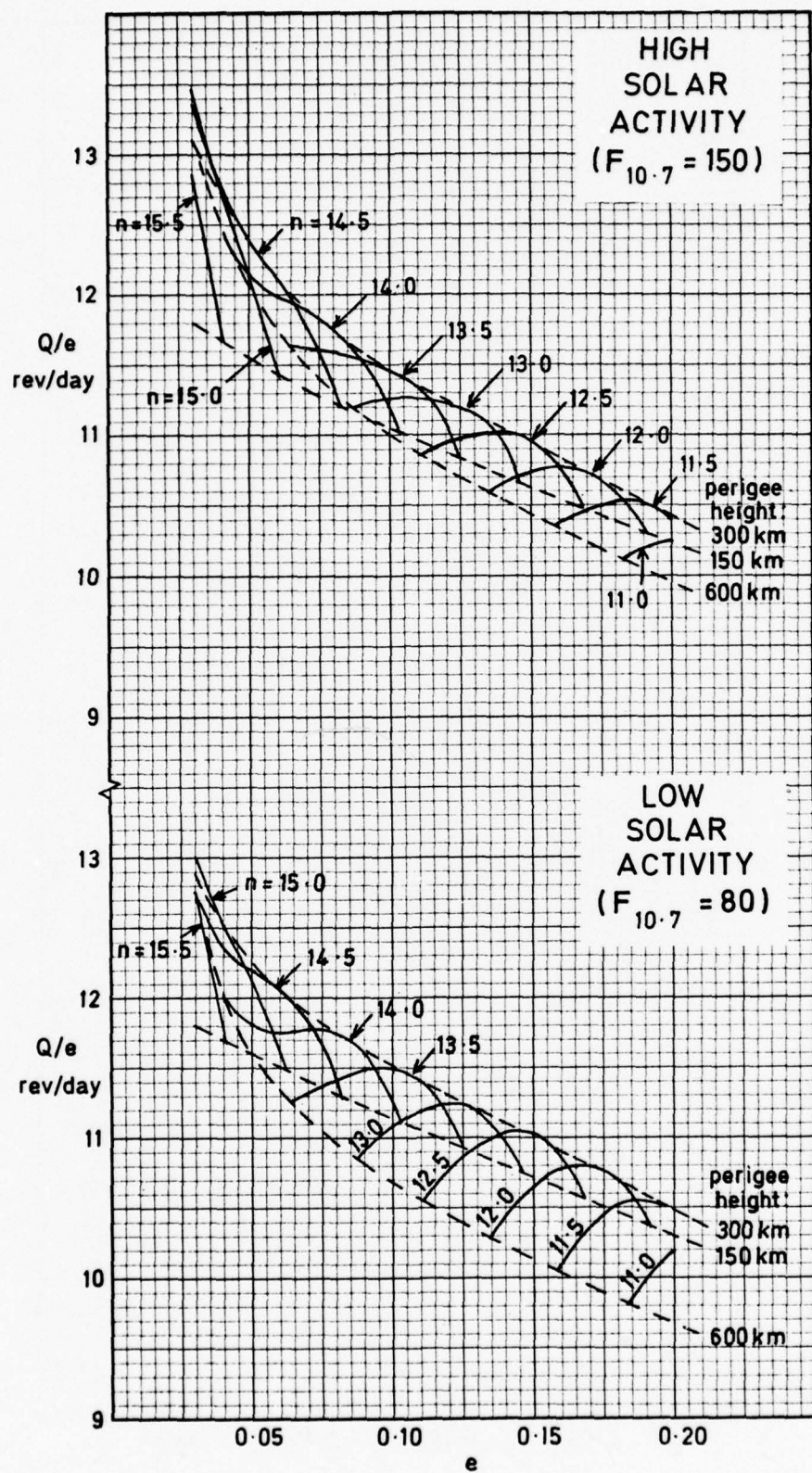


Fig 8 Variation of  $Q/e$  with  $e$  for  $0.03 \leq e \leq 0.2$ , with  $\mu$  from Fig 1

Fig 9

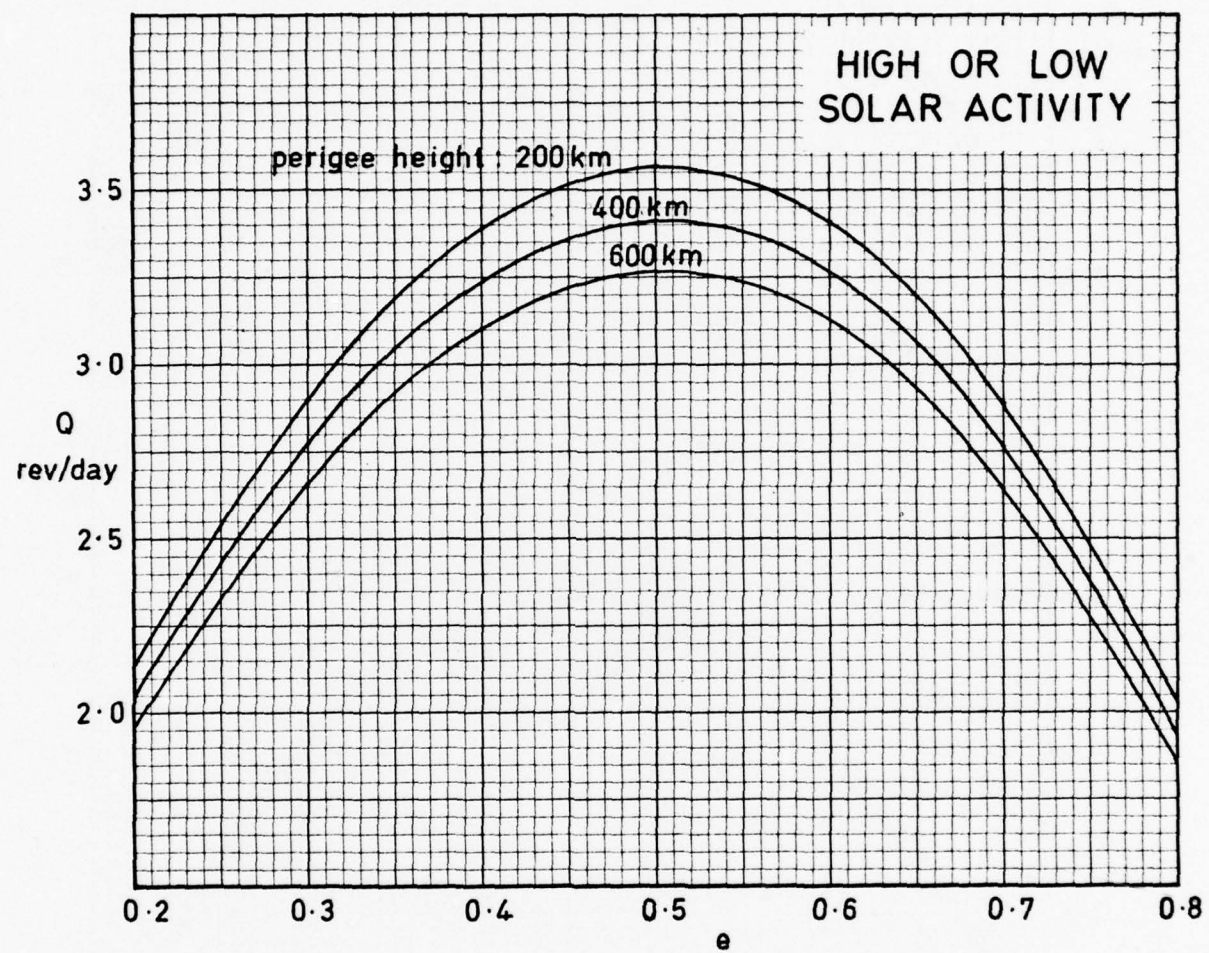


Fig 9 Variation of  $Q/e$  for  $0.2 \leq e \leq 0.8$ , with  $\mu = 0.1$

Fig 10

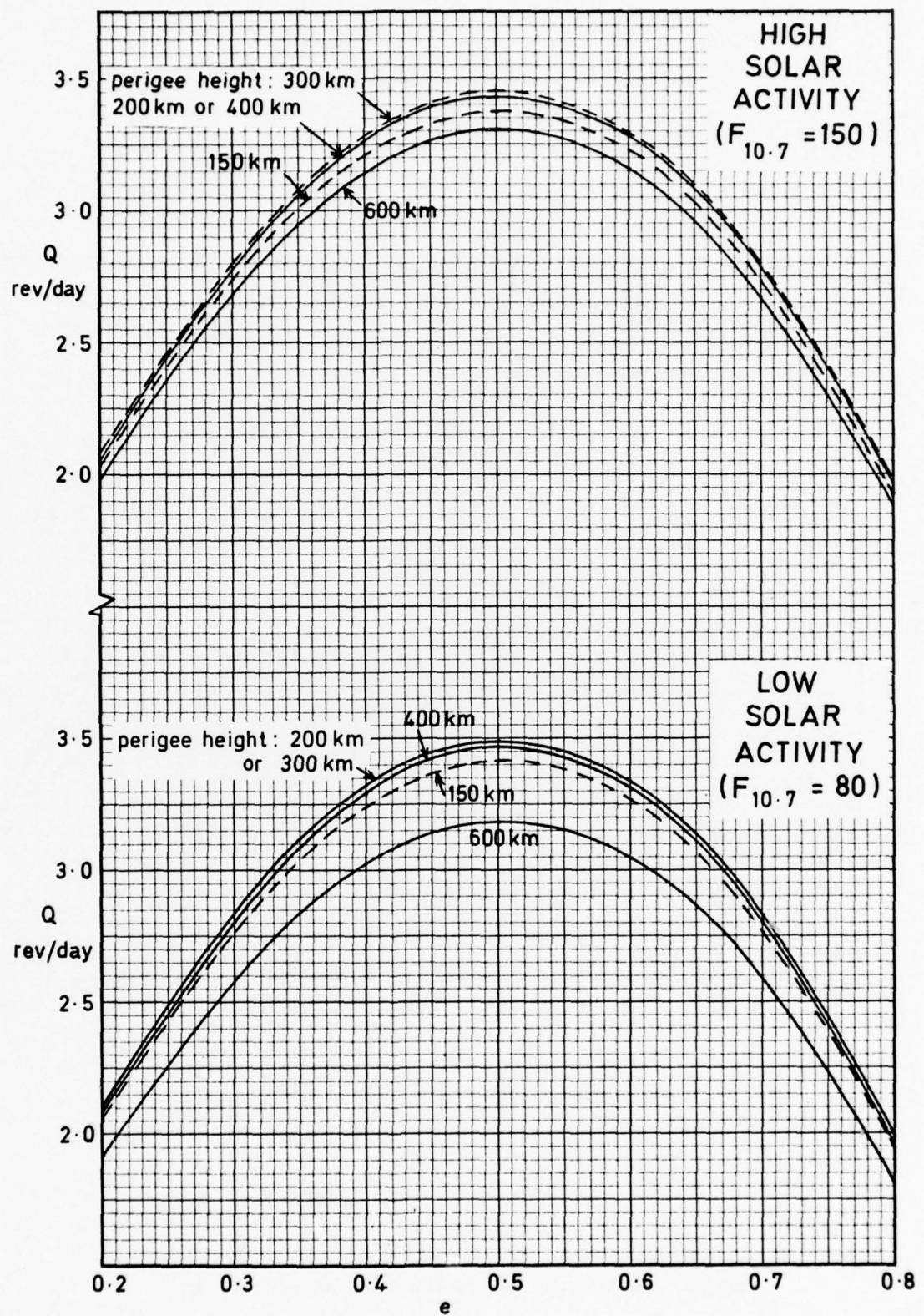


Fig 10 Variation of  $Q$  with  $e$  for  $0.2 \leq e \leq 0.8$ , with  $\mu$  from Fig 1

Fig 11

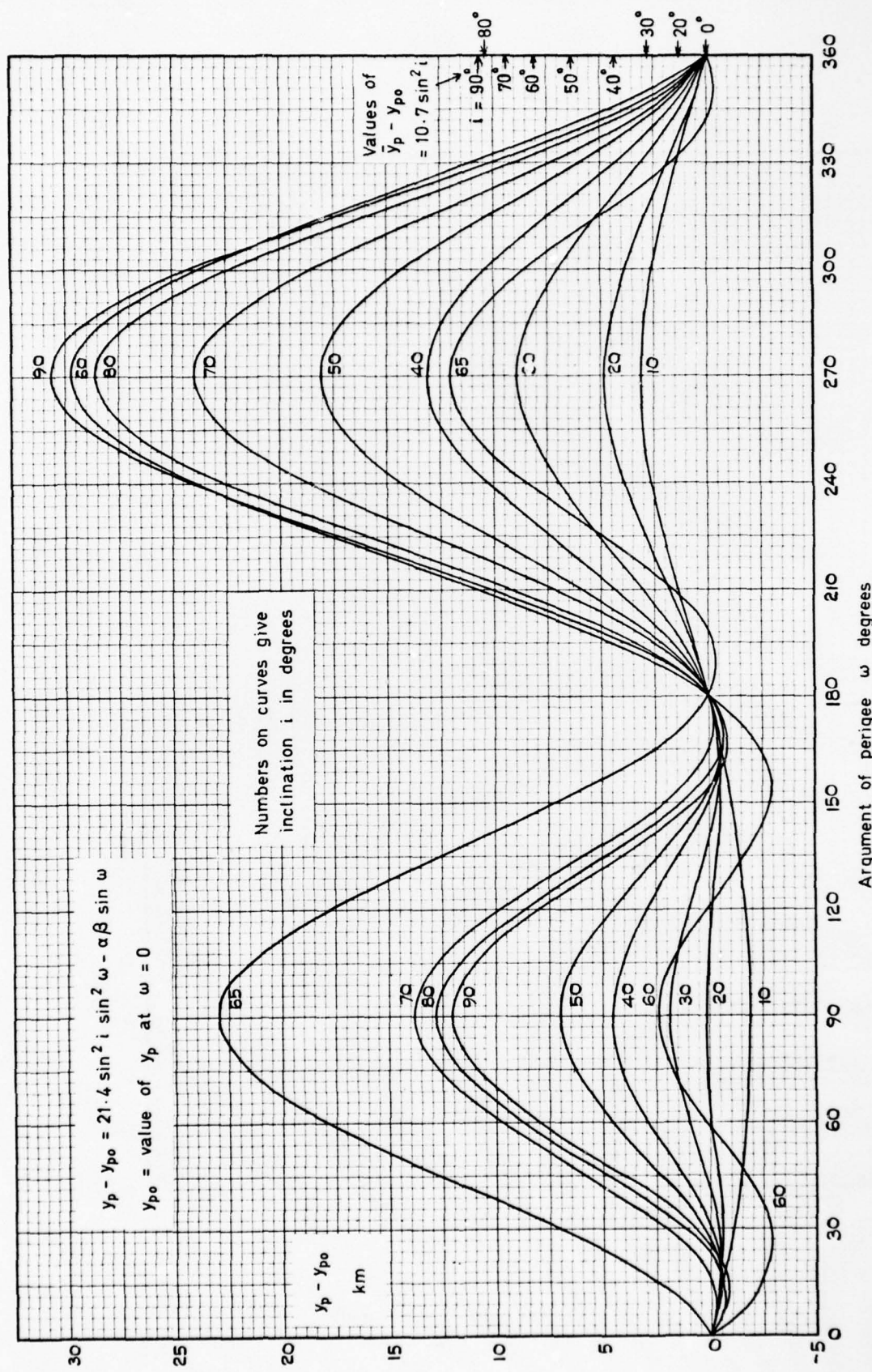


Fig 11 Variation of perigee height  $y_p$  due to Earth's oblateness and odd harmonics

Fig 12

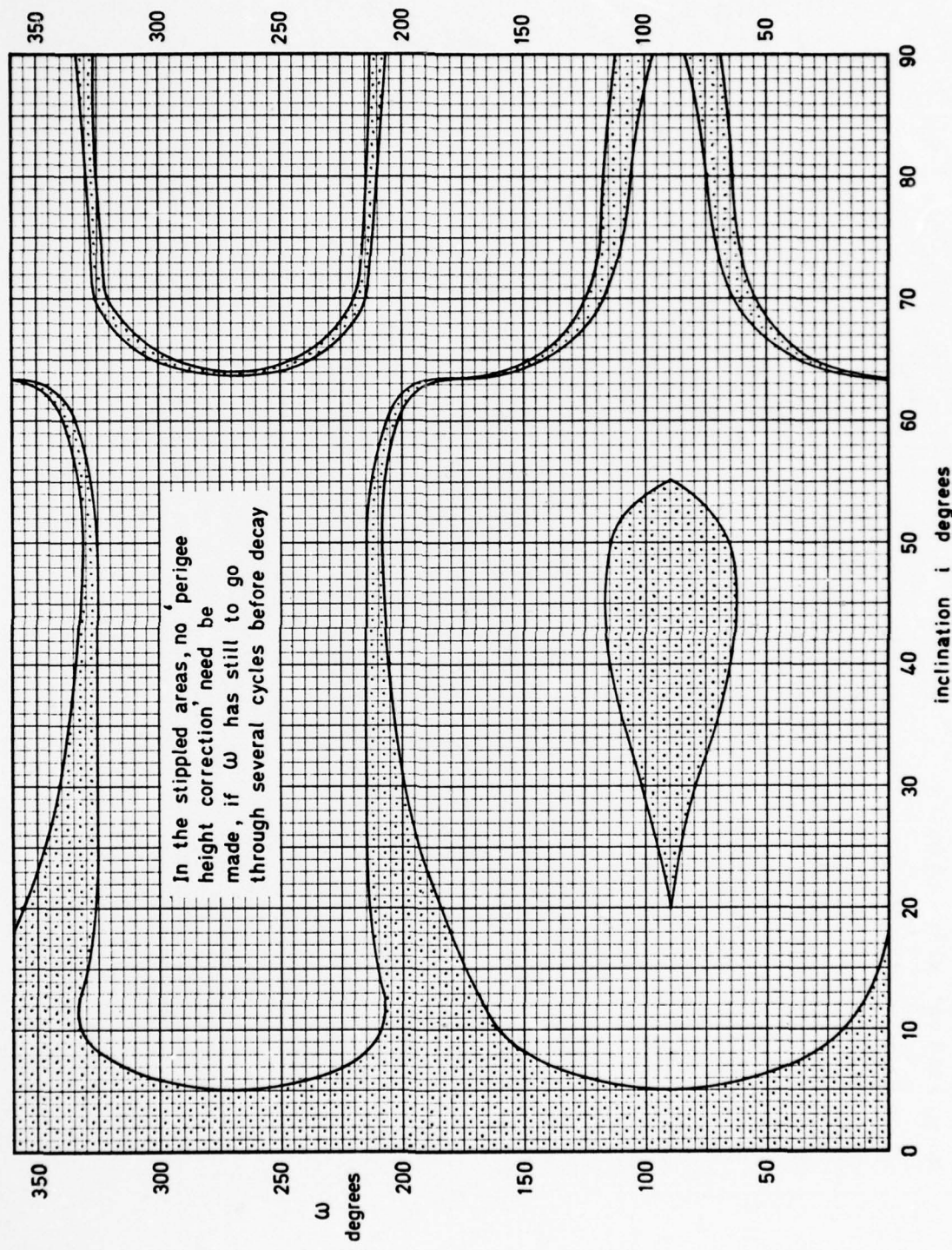


Fig 12 'Safe areas' for  $\omega$  (stippled)

Fig 13

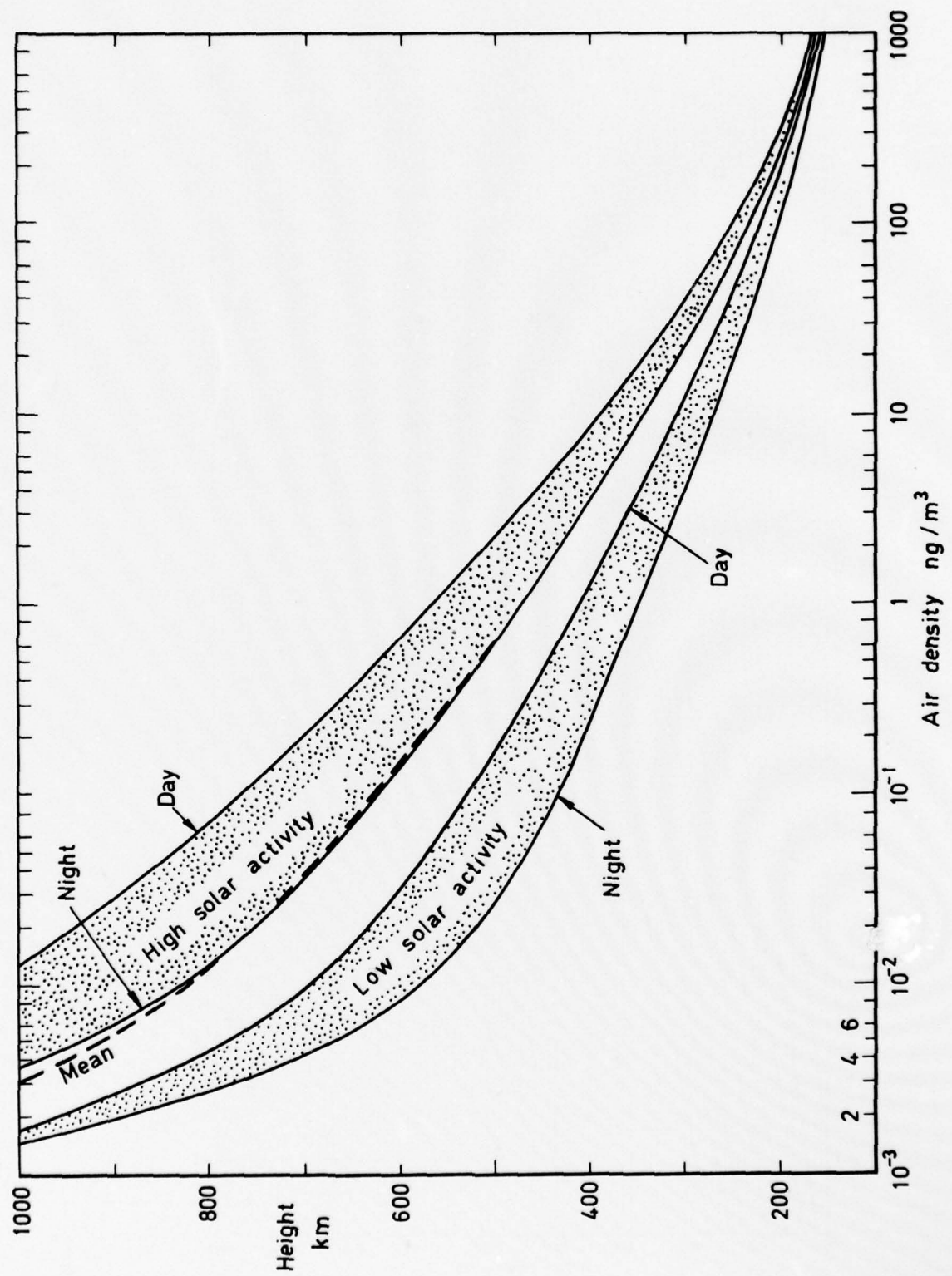


Fig 13 Variation of density with height for low and high solar activity, and the mean over a solar cycle

Fig 14

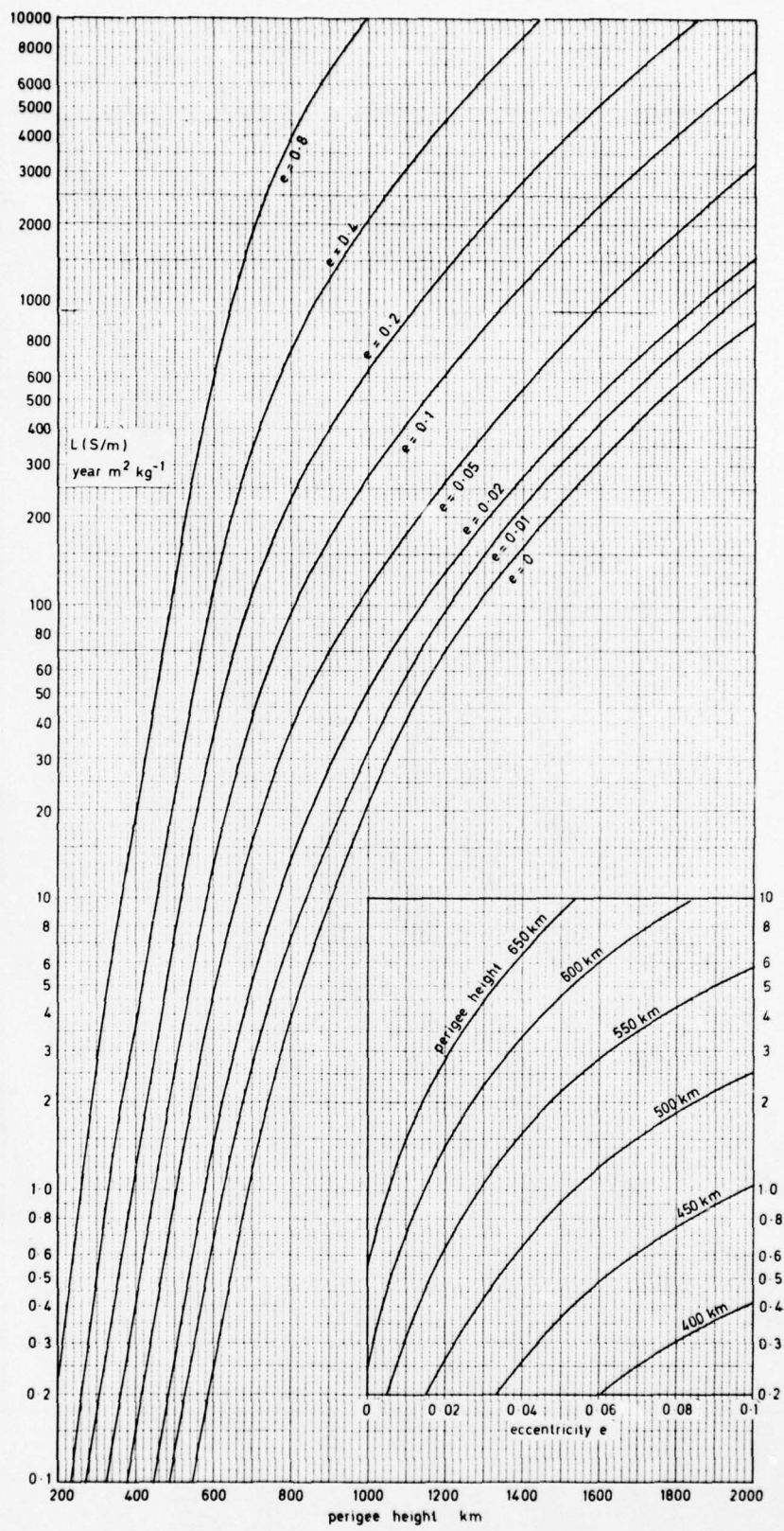


Fig 14      Lifetimes of long-lived satellites, based on mean density over an average solar cycle

Fig 15

Key to the numbers:

1. 1969 - 08B length 7.5 m
2. 1969 - 19A length 8.0 m
3. 1969 - 26A length 8.0 m
4. 1969 - 33B length 8.0 m
5. 1969 - 16B length 1.5 m
6. 1969 - 24B length 7.4 m
7. 1969 - 25E length 2.05 m
8. 1969 - 84B length 3.8 m
9. 1970 - 25C length 6.0 m
10. 1969 - 43B length 18.7 m
11. 1968 - 103B length 12 m
12. 1969 - 69B length 8.6 m
13. 1969 - 77B length 8.0 m
14. 1970 - 13D length 2.0 m
15. 1970 - 109B length 1.6 m
16. 1973-27B length 24.8 m

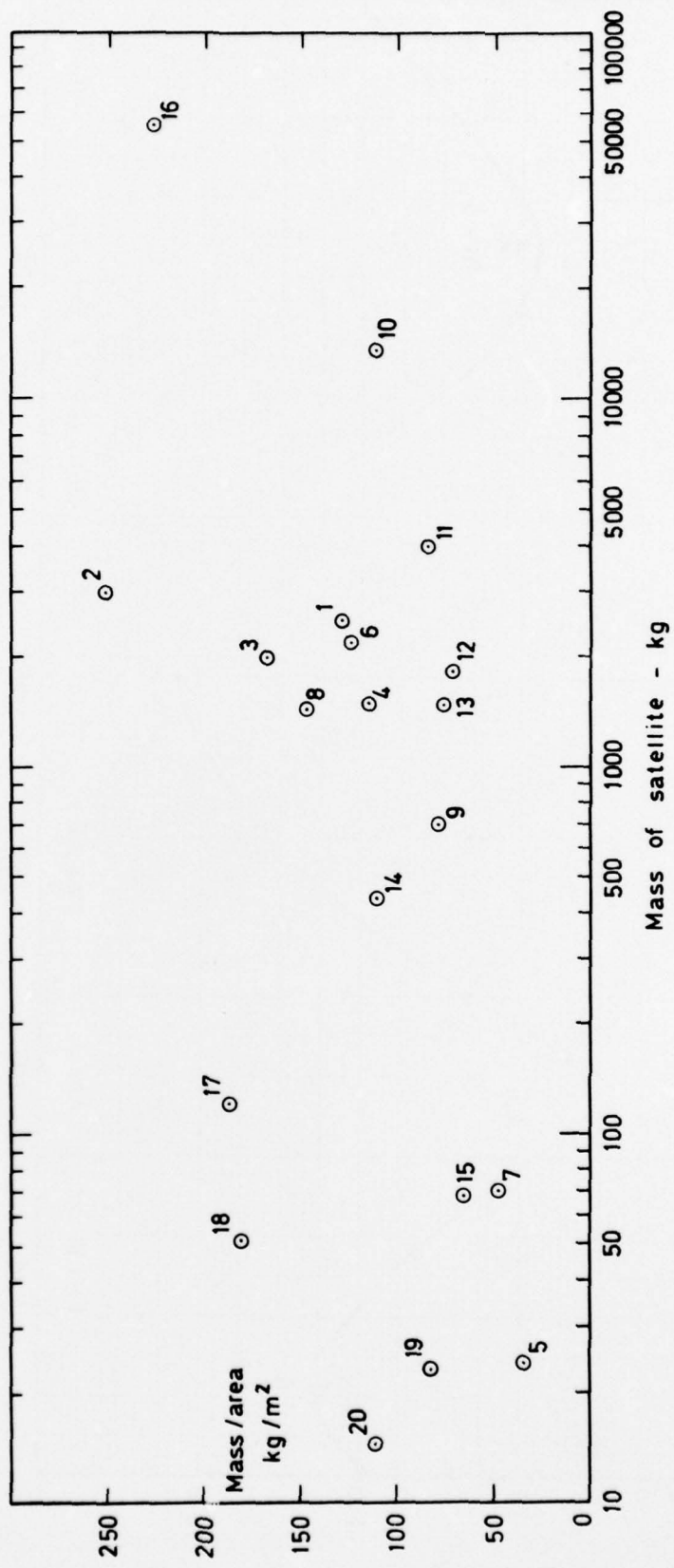


Fig 15 Effective mass/area ratios m/S for a wide selection of satellites

Fig 16

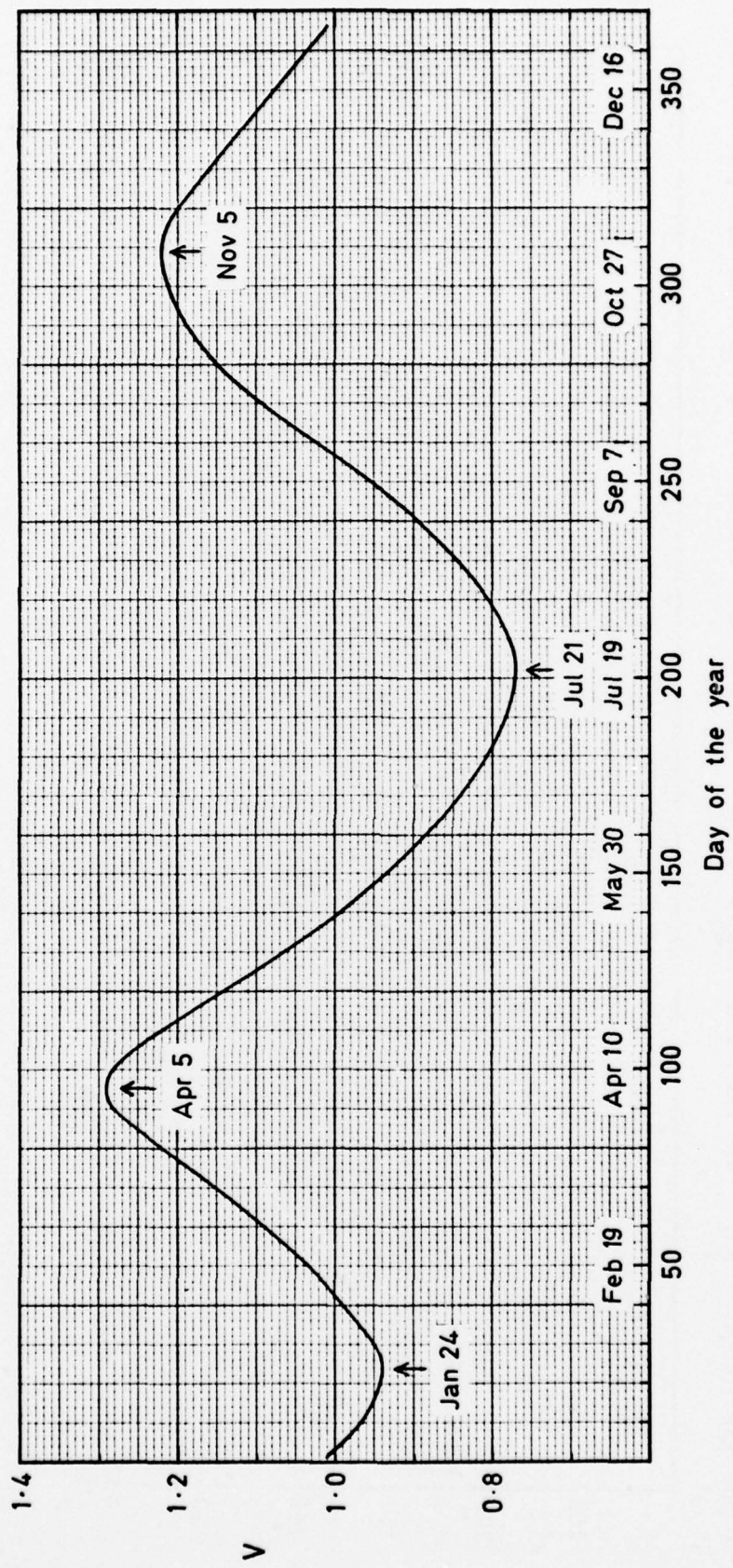


Fig 16 Semi-annual variation  $V$  recommended by Walker 19 for heights of 200-250 km

Fig 17

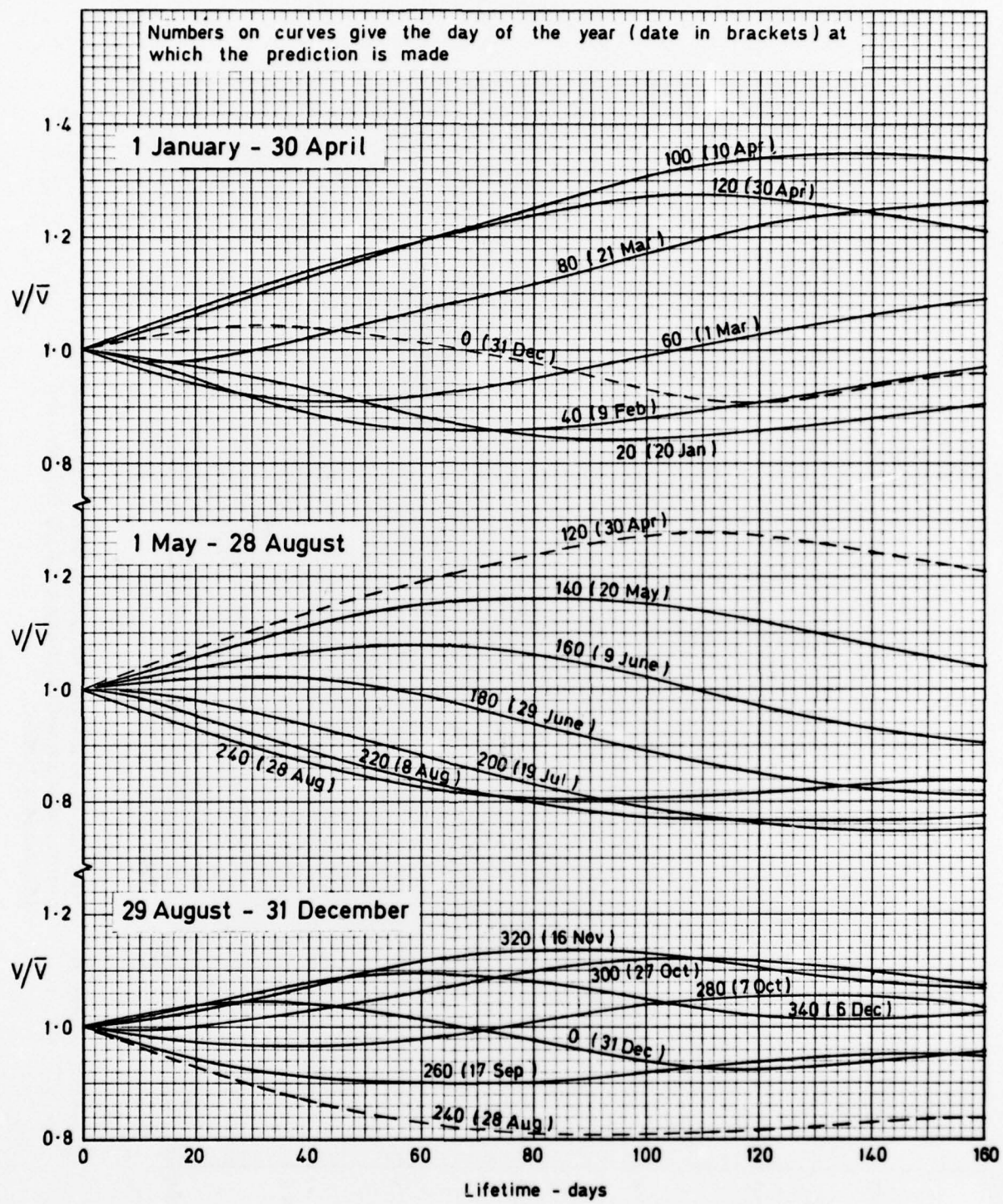
Fig 17 Variation of semi-annual correction factor  $V/\bar{V}$  with lifetime

Fig 18

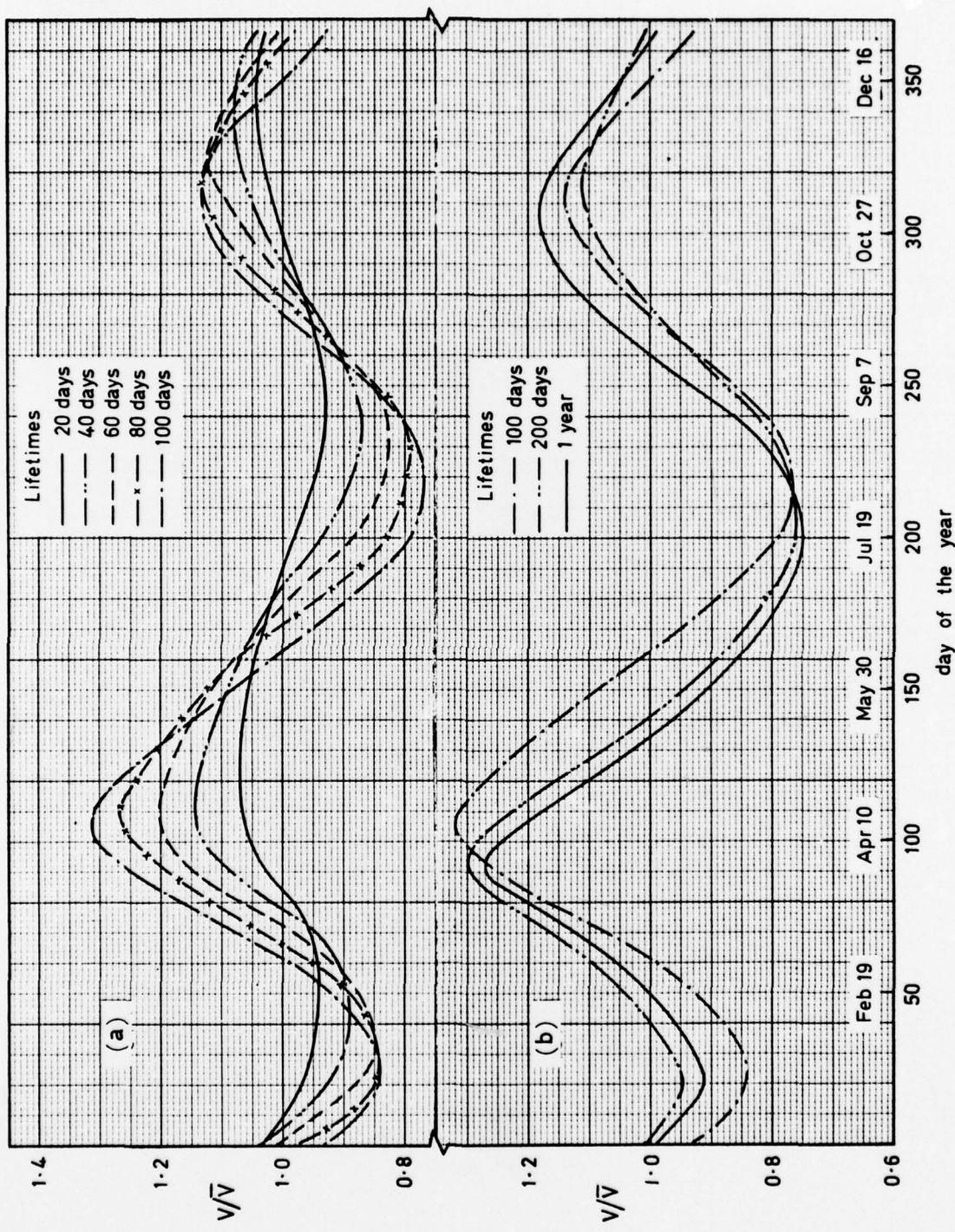


Fig 18 Variation of semi-annual correction factor  $V/\bar{V}$  during the year for satellites with lifetimes of (a) 20-100 days and (b) 100 days-1 year

Fig 19

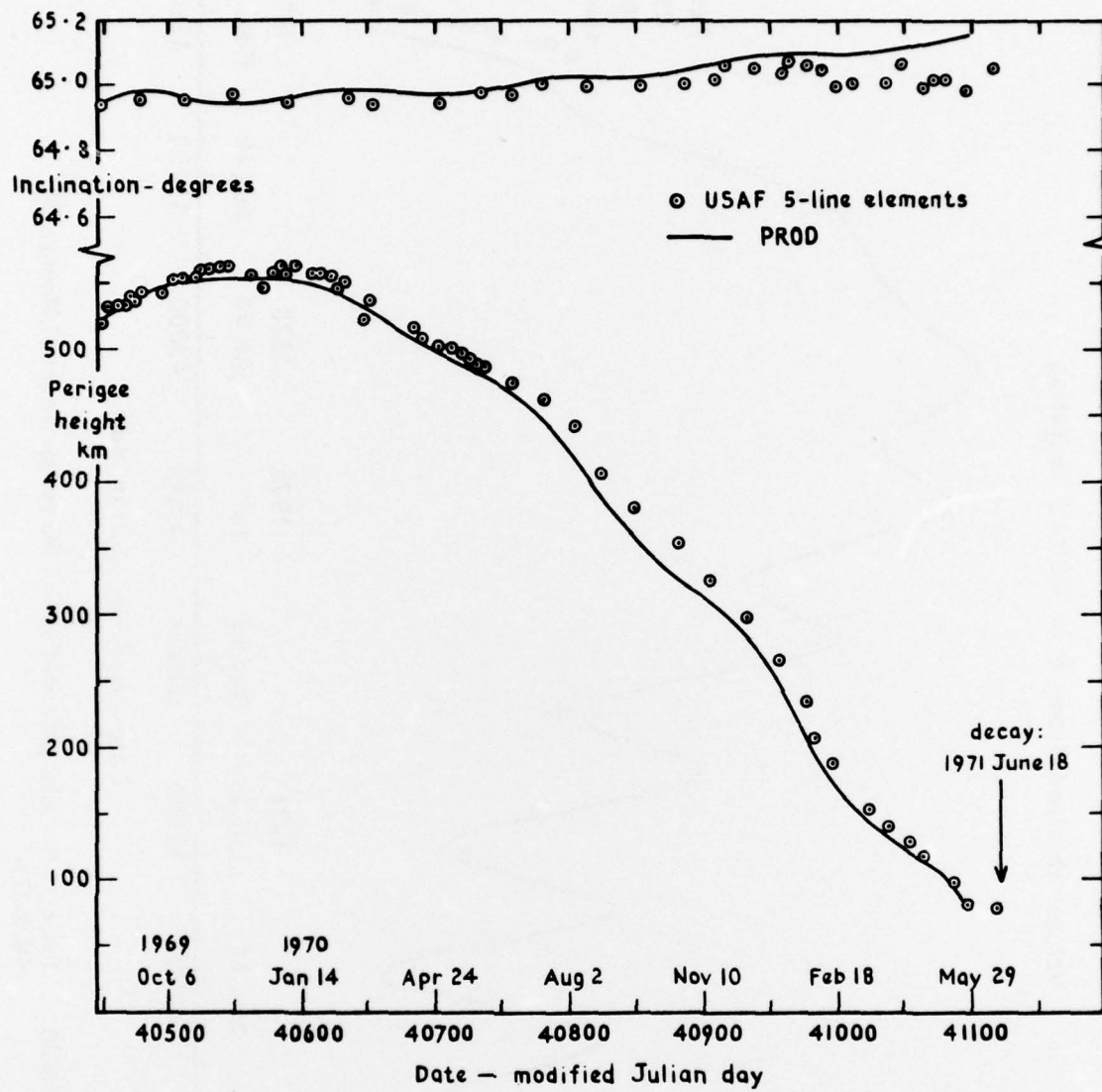


Fig 19 Variation of perigee height and inclination for Molniya 1M, 1969-61A, as given by PROD and USAF elements

Fig 20

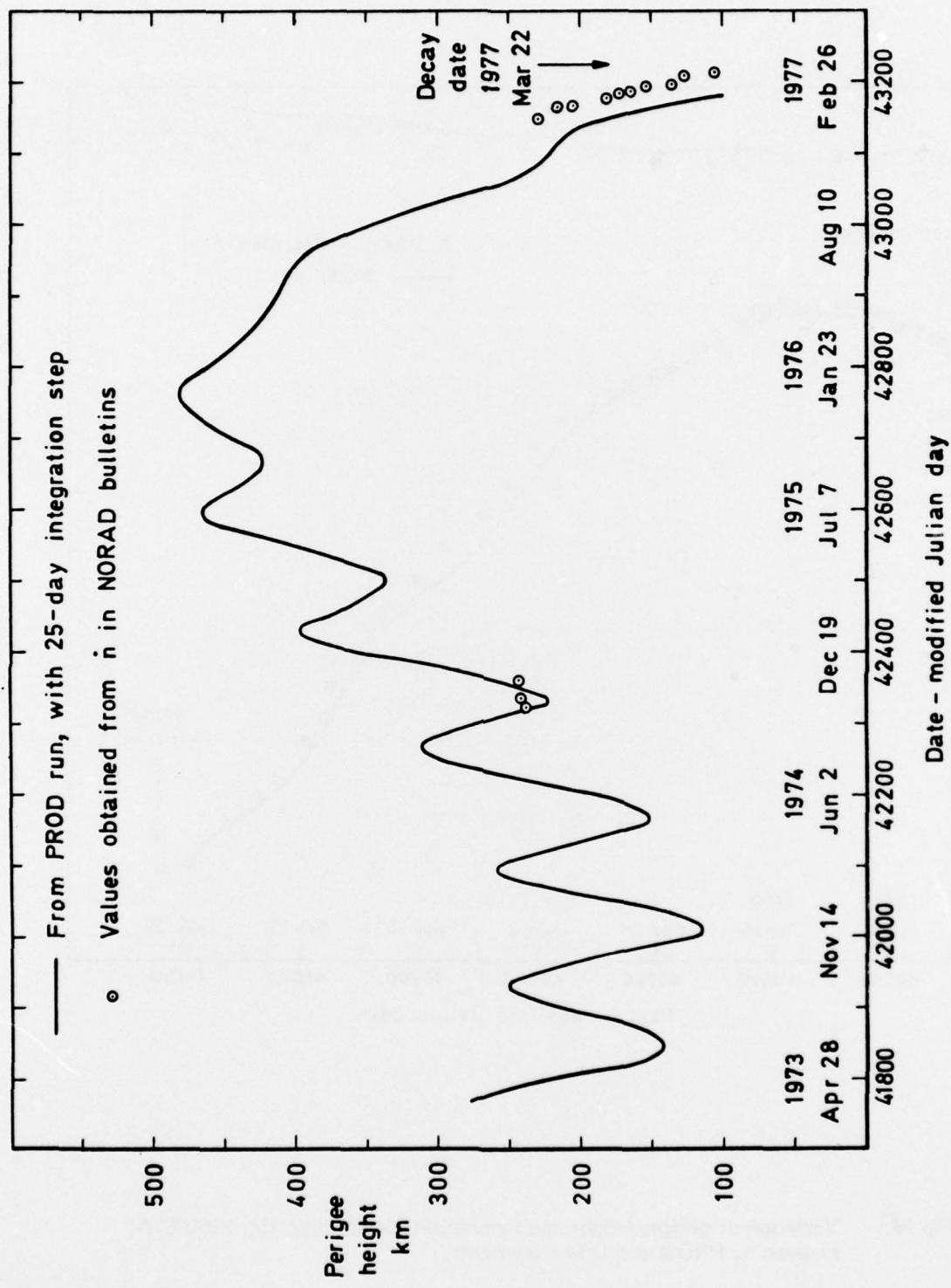


Fig 20 Effect of lunisolar perturbations on the perigee height of Molniya 2B, 1972-37A

Fig 21

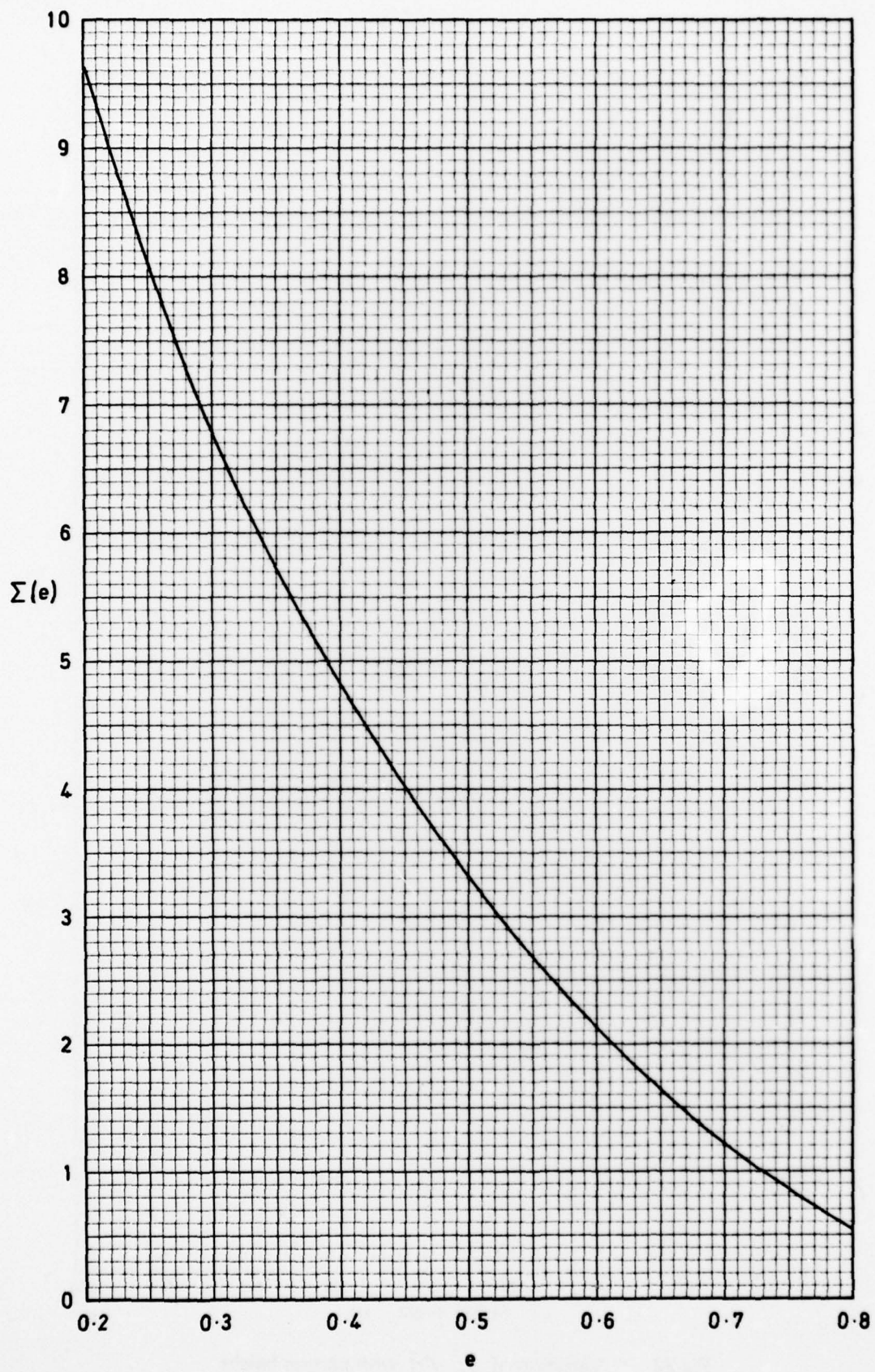


Fig 21 Variation of  $\Sigma(e)$  with  $e$

Fig 22

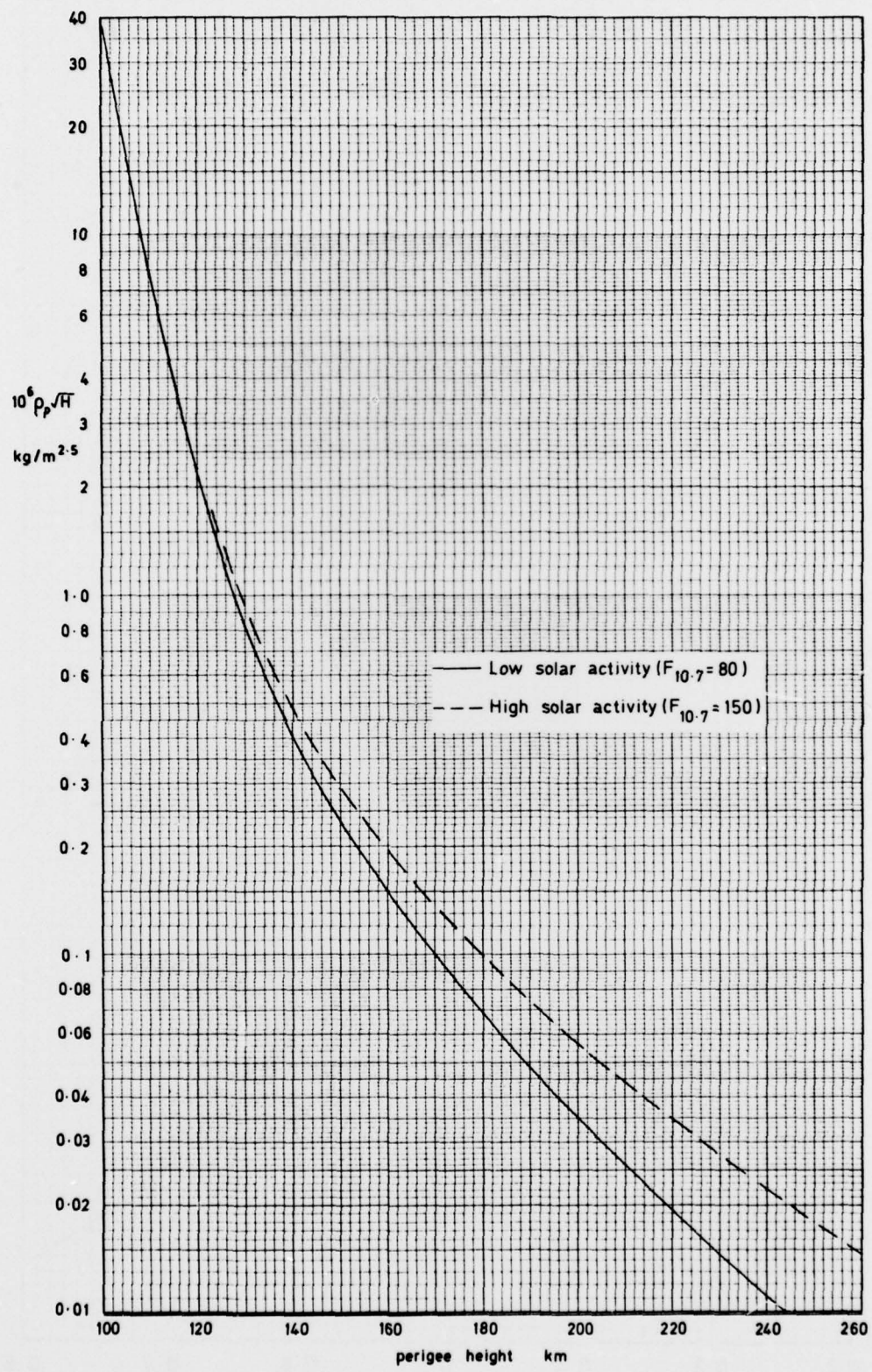


Fig 22 Variation of  $\rho_p \sqrt{H}$  with perigee height

Fig 23

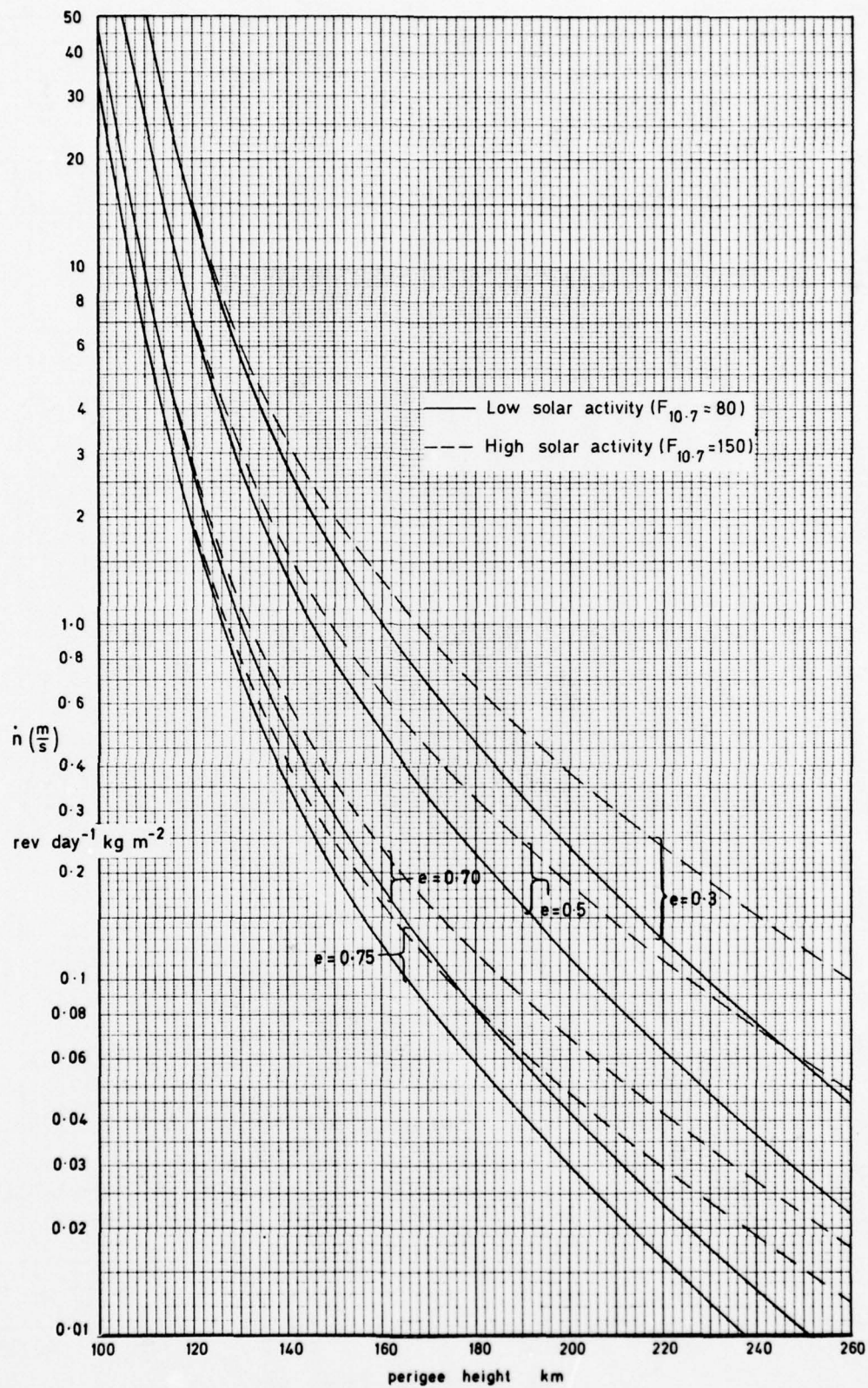


Fig 23 Variation of  $n \left( \frac{m}{s} \right)$  with perigee height for specified values of  $e$

Fig 24

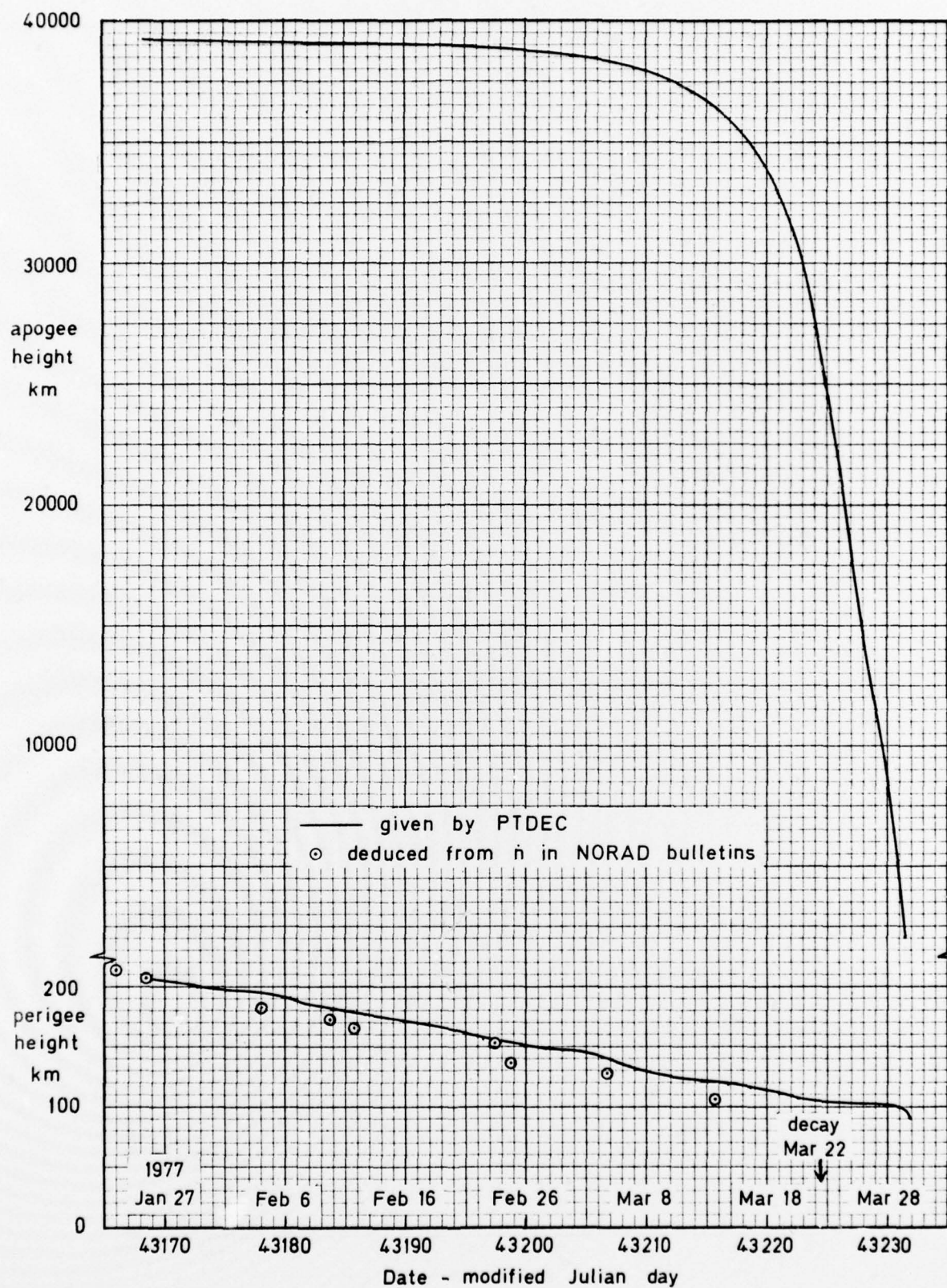


Fig 24 Perigee and apogee height of Molniya 2B, 1972-37A, during its last two months in orbit

Fig 25

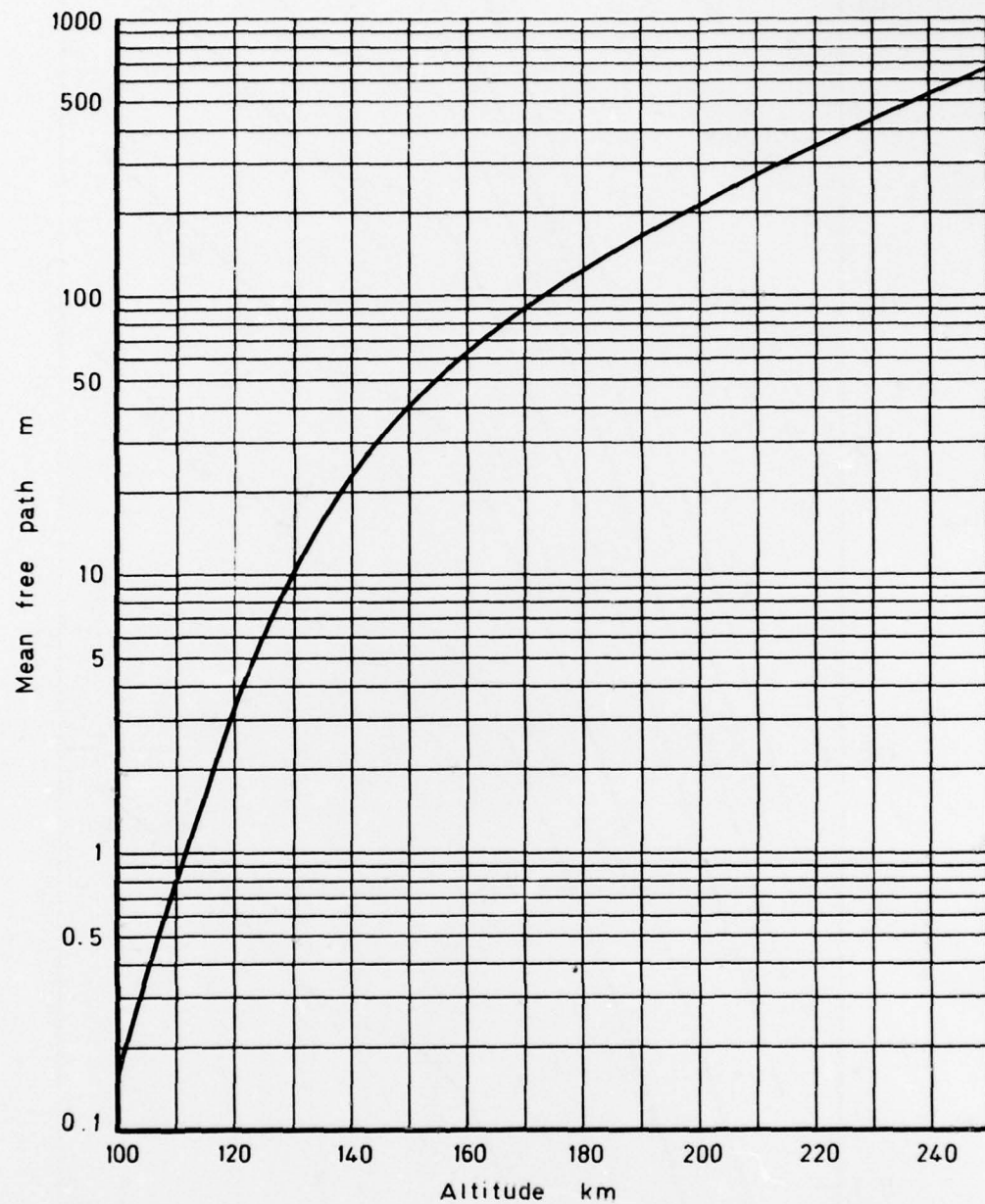


Fig 25      Atmospheric mean free path for heights between 100 and 250 km,  
as given by the US Standard Atmosphere, 1962

Fig 26

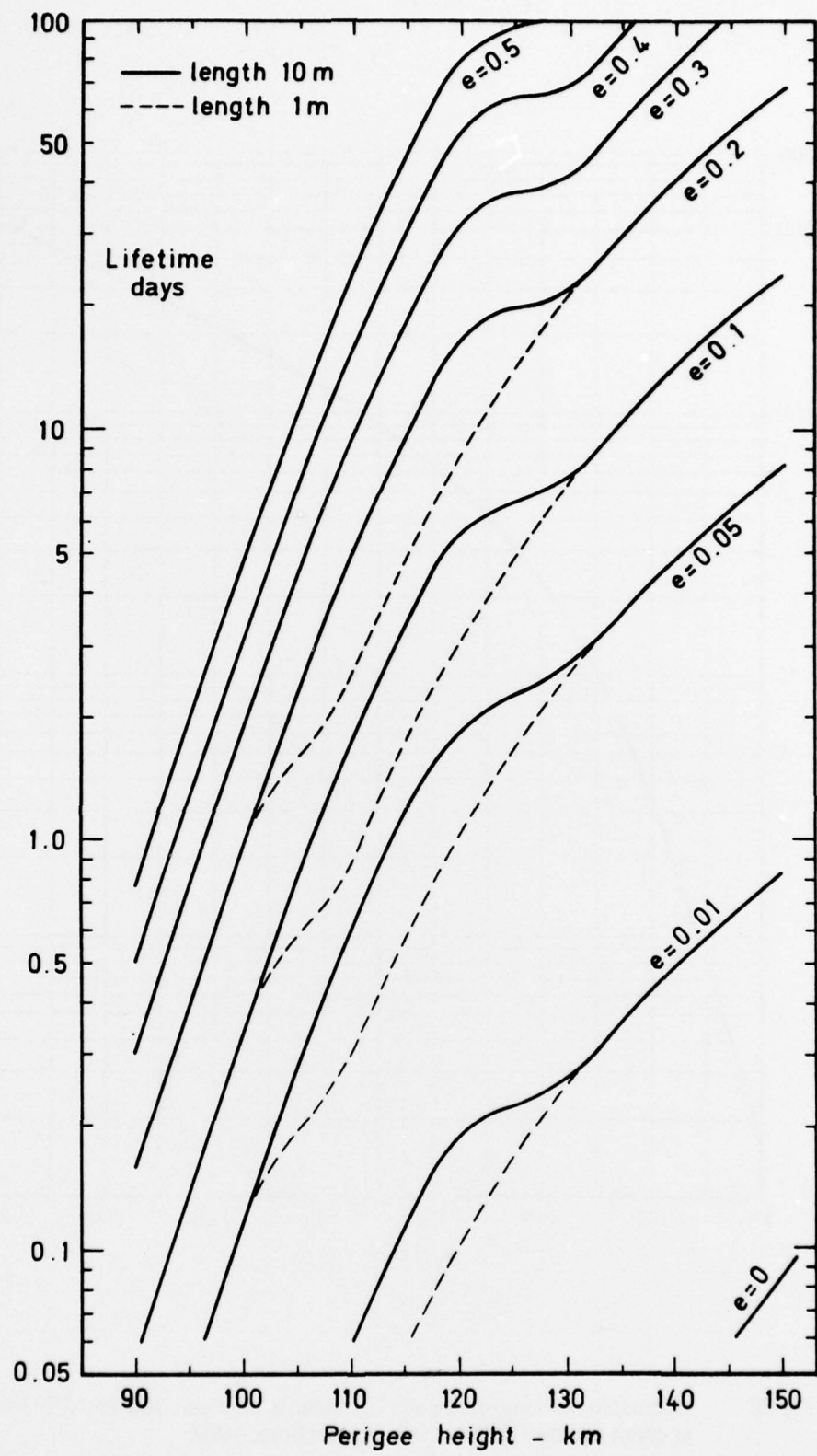


Fig 26 Lifetimes of satellites with mass/area  $100 \text{ kg/m}^2$ , and perigee height  $< 150 \text{ km}$

## REPORT DOCUMENTATION PAGE

Overall security classification of this page

UNCLASSIFIED

As far as possible this page should contain only unclassified information. If it is necessary to enter classified information, the box above must be marked to indicate the classification, e.g. Restricted, Confidential or Secret.

1. DRIC Reference (to be added by DRIC)	2. Originator's Reference RAE TR 77111	3. Agency Reference N/A	4. Report Security Classification/Marking UNCLASSIFIED
5. DRIC Code for Originator 850100	6. Originator (Corporate Author) Name and Location Royal Aircraft Establishment, Farnborough, Hants, UK		
5a. Sponsoring Agency's Code N/A	6a. Sponsoring Agency (Contract Authority) Name and Location N/A		
7. Title Methods for predicting satellite orbital lifetimes.			
7a. (For Translations) Title in Foreign Language			
7b. (For Conference Papers) Title, Place and Date of Conference			
8. Author 1. Surname, Initials King-Hele, D.G.	9a. Author 2	9b. Authors 3, 4 ....	10. Date July 1977   Pages 54   30 Refs.
11. Contract Number N/A	12. Period N/A	13. Project	14. Other Reference Nos. Space 532
15. Distribution statement (a) Controlled by - <b>RAE/Space</b> (b) Special limitations (if any) -			
16. Descriptors (Keywords) (Descriptors marked * are selected from TEST) Orbits. Satellite lifetimes. Orbital perturbations. Orbit decay.			
17. Abstract The accurate prediction of satellite decay dates some months or years ahead remains one of the most difficult and intractable problems of orbital mechanics, chiefly because the lifetime depends strongly on the future variations in air density, which are at present not accurately predictable.  In this paper simple graphical methods are presented for estimating the future lifetime of an Earth satellite from its current rate of decay, using theory adapted to an atmosphere with a realistic variation of density with height. The effects of the departure of the Earth and atmosphere from spherical symmetry, and the variations of density with time, are approximated by specifying correction factors. Orbits which experience serious lunisolar perturbations call for numerical integration methods, and the uses of the computer programs PROD and PTDEC are described.  Despite the many uncertainties, the remaining lifetimes of most satellites should be predictable with an accuracy of $\pm 10\%$ by these methods, which are based on many years' experience in making the monthly decay predictions for the RAE Table of satellites.			